Research Highlight

[FY2022]

Japan International Research Center for Agricultural Sciences

Meeting global challenges through research and technology development

国際農研

Greenhouse gas emission factor value from Vietnamese beef cattle manure sun-drying process

Livestock manure and its management process are known to be a major source of greenhouse gas (GHG) emissions. Developing countries, including some SE Asian countries, sometimes do not have their own emission factor (EF) values, which forces them to use the Tier 1 approach with the default EF values provided by the IPCC to estimate their GHG inventory. Therefore, some GHG emission measurement dataset is needed to develop the independent EF values for higher Tiers estimation. Here, we conducted a farm survey in southern Vietnam to identify the major manure management system in the region. Moreover, we measured the GHG emission from the sun-drying system, estimated the EF value for this specific management, and focused on the manure microbiome to analyze its relationship with GHG emissions.

A questionnaire-based farm survey was conducted among 20 beef cattle farmers in Ben Tre province, which has a high cattle population in the Mekong Delta region, to identify the major manure management system in the region. We found that most farmers sun-dry the manure in their backyards (Fig. 1). We carried out the sun-drying experiment of beef cattle manure by mimicking the local practice and found that significant fresh weight loss occurs within 3-4 days (Fig. 2A). We measured the GHG emissions and found that CH_4 emission occurs only at the beginning, while N_2O emission was negligible (Figs. 2B, 2C). The potential EF values from this management category were estimated as CH_4: 0.295 ± 0.078 g kg^{-1}VS and N_2O: 0.132 ± 0.136 g N_2O-N kg^{-1} $N_{initial}$, respectively. We estimated the function of the microbiome and elucidated that sun-drying treatment significantly reduces the activity of methane-related metabolism at the beginning stage (p<0.001), which is reflected by the significant reduction in the relative abundance of the methanogens (Fig. 3B), and this agrees well with the significant reduction in methane emission at the beginning of drying (Figs. 2B and 2C). On the other hand, the effect of sun-drying on N conversion activity, which includes nitrification or denitrification, was not statistically significant (p=0.563, Fig. 3C).

This information can be utilized as the EF value for the Vietnamese national GHG inventory. Sun-drying systems can be said to be very effective in manure management from the point of view of CH_4 emission mitigation. Other agricultural practices that produce GHGs, such as dried manure application to coffee/pepper farmlands, should be further investigated.

(K. Maeda,
T.V. Nguyen [Institute of Agricultural Science for Southern Viet Nam (IASVN)],
T.H.T. Nguyen [IASVN], V.N. La [IASVN], T. Suzuki [National Agriculture and Food Research Organization (NARO)], D.D. Nguyen [Tay Nguyen University, Vietnam])

Fig. 1. Sun-drying of beef cattle manure in Ben Tre province

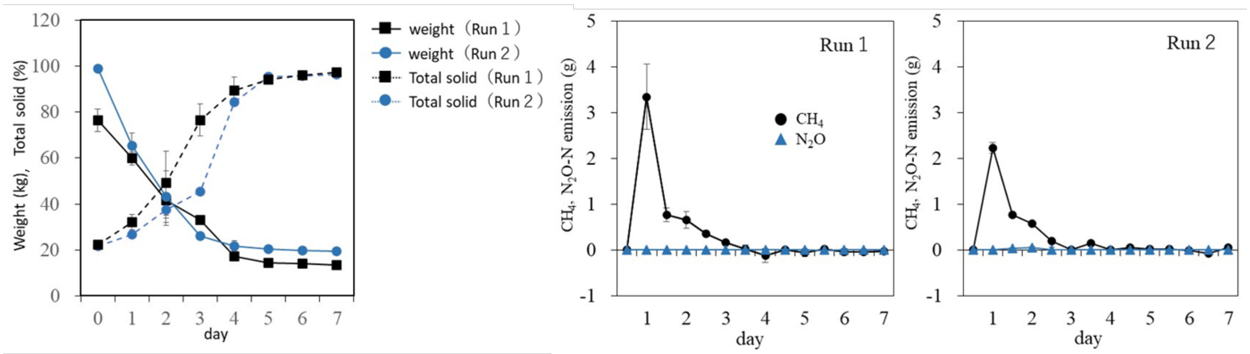

Fig. 2. Change in fresh weight, total solids, and GHG emissions from manure sun-drying

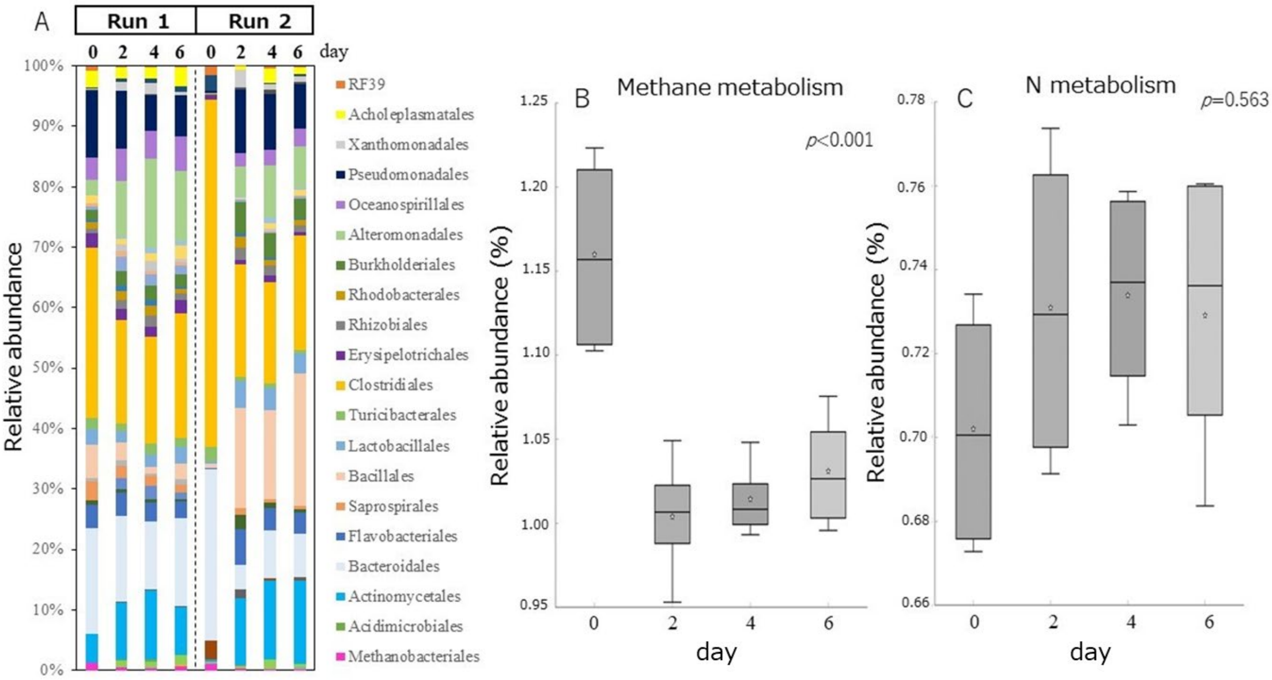

Fig. 3. Change in the manure microbiome and its functions during sun-drying

Reference: Nguyen et al. (2022) *PLoS ONE* 17(3): e0264228.
Figures reprinted/modified with permission.

A comprehensive assessment of greenhouse gas emissions from Thai beef cattle production

Livestock is known to be a major source of greenhouse gases (GHGs). However, a GHG emission dataset from livestock production in Southeast Asian countries is still lacking. There is a strong need for a CH_4 conversion factor（*Ym* value）dataset or emission factor (EF) value for each manure management category. Moreover, some developed countries have independent datasets, while no dataset covers both. Here, we provide the dataset that covers both enteric CH_4 and GHG emissions during manure storage from a Thai native beef cattle production system. In addition, we assess the effect of mixing rice straw (RS), which is an abundant and ready-to-use resource.

Four Thai native cattle were fed a restricted amount (2% of BW) of a diet comprised of 70% Pangola grass and 30% commercial concentrate to meet their digestible energy requirements. The emission of enteric CH_4 was measured by the head-hood system for 6 days in three periods, and the manure was accumulated in the dynamic chamber system coupled with GC-FID and ECD. Five hundred kg of manure with and without 25 kg of rice straw mixture were put in the chamber for 12 weeks and mixed every 2 weeks. Dry matter (DM) intake for runs 1 and 2 was 5.4 and 5.6 kg/d, while DM digestibility was 53.68 and 55.42%, respectively. Digestibility of organic matter, crude protein, and ether extract was also in the range of typical values for the region. The *Ym* value was 6.87%GEI (gross energy intake) and CH_4 emission from manure storage was 0.68％GEI (Table 1). Mixing of RS significantly affected manure temperature, reaching 65.1°C–66.2°C in the RS mixed pile while that of the control pile ranged between 43.8°C and 47.4°C (Fig. 1). There was a high variation in the gas emission; the CH_4 emission from the RS mixed pile showed a lower tendency while there was no significant effect on the total CH_4 emission (Fig. 2A). The same trend was observed for N_2O emission (Fig. 2B). An analysis of the relationship between the estimated function of manure microbiome and GHG emission shows that a significant treatment effect was obtained on methane metabolism at the beginning (Fig. 3), and it agrees well with the mitigation of the peak CH_4 emission in the RS mixed manure (Fig. 4).

This information can be utilized as the EF value for Thailand’s national GHG inventory. The use of rice straw as a bulking agent can enhance OM degradation in the manure and suppress the activity of methanogens, but it should be noted that its effect may be limited for small-scale farmers with small amounts of manure.

(K. Maeda, Y. Cai,
W. Angthong [Ruminants Feeding Standard Research and Development Center (RFSDC), Thailand], O. Kaeokliang [RFSDC], S. Kamphayae [RFSDC]
T. Suzuki [NARO], A. Mori [NARO], H. Kitwetchroen [Khon Kaen University, Thailand])

Table 1 . Fate of the energy contained in the feedstuff（kJ/head/day)

	Run 1	Run 2	%
Gross Energy Intake	90,754.4	99,609.8	100.00
Retained energy	20,166.6	16,614.9	19.32
Heat production	24,407.6	29,588.3	28.36
Enteric CH_4	6,161.2	6,918.6	6.87
Urine	1,197.0	1,785.0	1.57
Manure (excluding CH_4 emission during storage)	38,032.4	44,201.0	43.20
CH_4 during manure storage	789.6	501.9	0.68

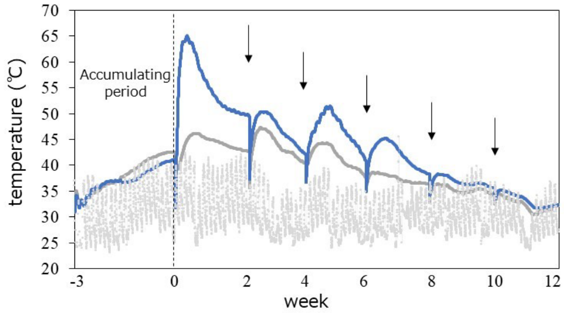

Fig. 1. Temperature profiles during manure storage

Blue: rice straw mixed

Grey: control

Light grey: ambient temperature

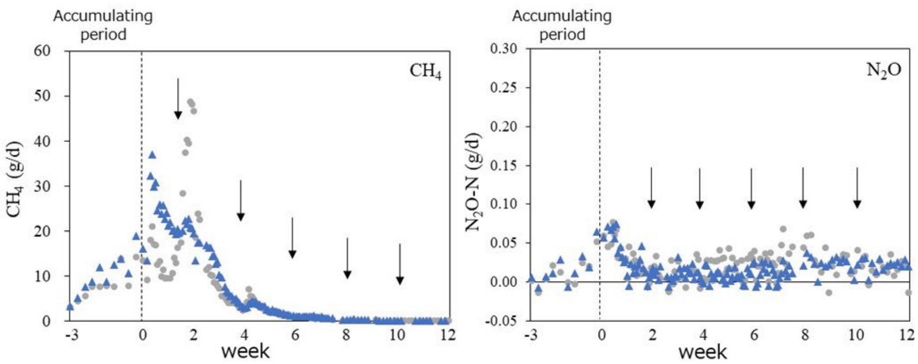

Blue: rice straw mixed

Grey: control

Arrows: turnings

Fig. 2. CH_4 and N_2O emissions during manure storage

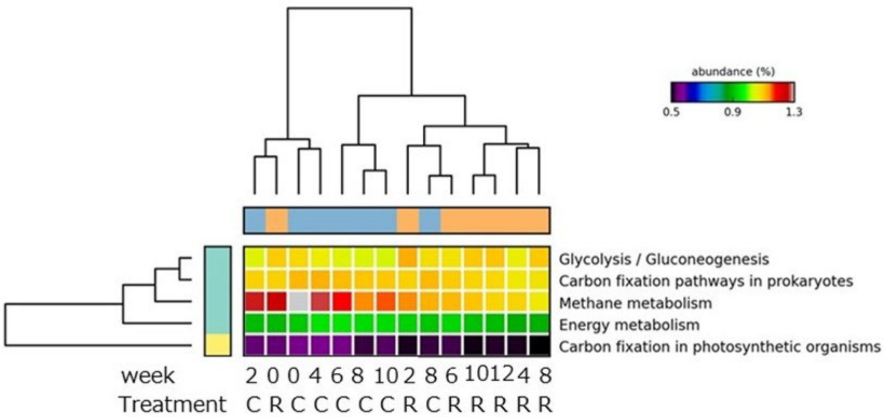

R: rice straw mixed

C: control

Fig. 3. Effect of rice straw mixing on functions of manure microbiome

Reference: Angthong et al. (2022) *Front. Environ. Sci.* 10: 872911.
Figures and table reprinted/modified with permission.

Enteric methane emission models for beef cattle in Southeast Asia

Ruminants are one of the major sources of greenhouse gas emissions. Therefore, a precise estimation of this category is needed. Since direct precise measurement from each cattle is labor-consuming and requires a specific expensive measurement facility, an alternative approach that enables indirect estimation with available data, such as the feed intake or its quality, is needed. Currently, methane emissions from ruminants in each country are estimated using the methane conversion value (Y_m), which utilizes the gross energy intake (GEI) data. However, the current model is composed of datasets from Western cattle breeds and feed composition, which is very different from the situation in Southeast Asian countries, and it makes the precision of the estimation poor. Therefore, a better estimation equation model that reflects the specific production condition in Southeast Asian countries is needed. Here, we revised the current methane emission equation model by collecting the available methane emission data and feed intake or its composition data across Southeast Asian countries.

We conducted a survey on methane emission data and feed intake or composition data from 8 Southeast Asian countries as part of the GRA-LRG global network project, and found that only 3 countries (Thailand, Vietnam, and Indonesia) possess methane emission data using the standard chamber method. After quality filtering, 398 data points were used for developing the methane emission estimation equation model. First, we developed the model based on dry matter intake data (Table 1, ①). The RMSPE value is lower compared to current IPCC Tier 2 (2019) or Global Network Tier 2 equation models, indicating that our model has higher precision compared to these existing models (Fig. 1). The RMSPE value could be further lowered by including NDF or body weight as additional parameters (Table 1, ②③, Fig. 1). Furthermore, the dataset was divided into 3 categories according to the roughage/concentrate ratio (all forage: 119, high forage: 163, low forage: 116), and they were used for developing higher precision equation models (Table 2). The RMSPE value was lowest for the high forage (50%–85%) category, which is the most widespread feed composition in the region.

These estimation equations can be utilized as a better and alternative approach compared to the existing estimation equations for inventory data development in each country. However, we need to keep in mind that the dataset used for the methane emission estimation equation model is derived from only a few countries (Thailand, Vietnam, and Indonesia).

(K. Maeda,
T. Suzuki [National Agriculture and Food Research Organization (NARO)],
Tee T.P. [University of Putra-Malaysia (UPM)], Liang J.B. [UPM], and 37 others

Table 1. Estimation equation and prediction error of methane emission from the rumen all data (n=398)

Model		RMSPE(%)
① DMI	20.15 (4.42) + 19.59 (0.90) x DMI	16.9
② DMI, NDF	36.03 (4.91) + 18.77 (0.86) x DMI – 0.34 (0.05) x NDF	15.2
③ DMI, NDF, BW	26.63 (4.82) + 15.20 (1.04) x DMI – 0.29 (0.05) x NDF + 0.08 (0.015) x BW	14.2
Global Network Tier 2	[0.061 x GEI] ÷ 0.05565	27.4
IPCC (2019) Tier 2	[0.07 x GEI] ÷ 0.05565	19.9
Suzuki et al. (2018)	8.91 + 22.71 x DMI	16.8
van Lingen et al. (2019)	54.2 + 12.6 x DMI	19.0

DMI: dry matter intake, NDF: neutral detergent fiber, CP: crude protein, EE: ether extract, BW: body weight, GEI: gross energy intake, RMSPE: root mean square prediction error, values in the parenthesis: standard error

Table 2. Estimation equation and prediction error of methane emission from the rumen, high forage content（50% – 85%, n=163）

Model		RMSPE(%)
① DMI	14.27 (6.00) + 19.75 (1.27) x DMI	15.1
② DMI, NDF	34.32 (6.78) + 19.81 (1.14) x DMI – 0.43 (0.09) x NDF	13.0
③ CP, EE, NDF, BW	63.33 (9.89) – 2.19 (0.54) x CP + 2.74(0.86) x EE – 0.36 (0.11) x NDF + 0.28(0.02) x BW	13.2
Global Network Tier 2	[0.061 x GEI] ÷ 0.05565	21.5
IPCC (2019) Tier 2	[0.07 x GEI] ÷ 0.05565	15.1
Suzuki et al. (2018)	8.91 + 22.71 x DMI	16.5
van Lingen et al. (2019)	54.2 + 12.6 x DMI	17.4

DMI: dry matter intake, NDF: neutral detergent fiber, CP: crude protein, EE: ether extract, BW: body weight, GEI: gross energy intake, RMSPE: root mean square prediction error, values in the parenthesis: standard error

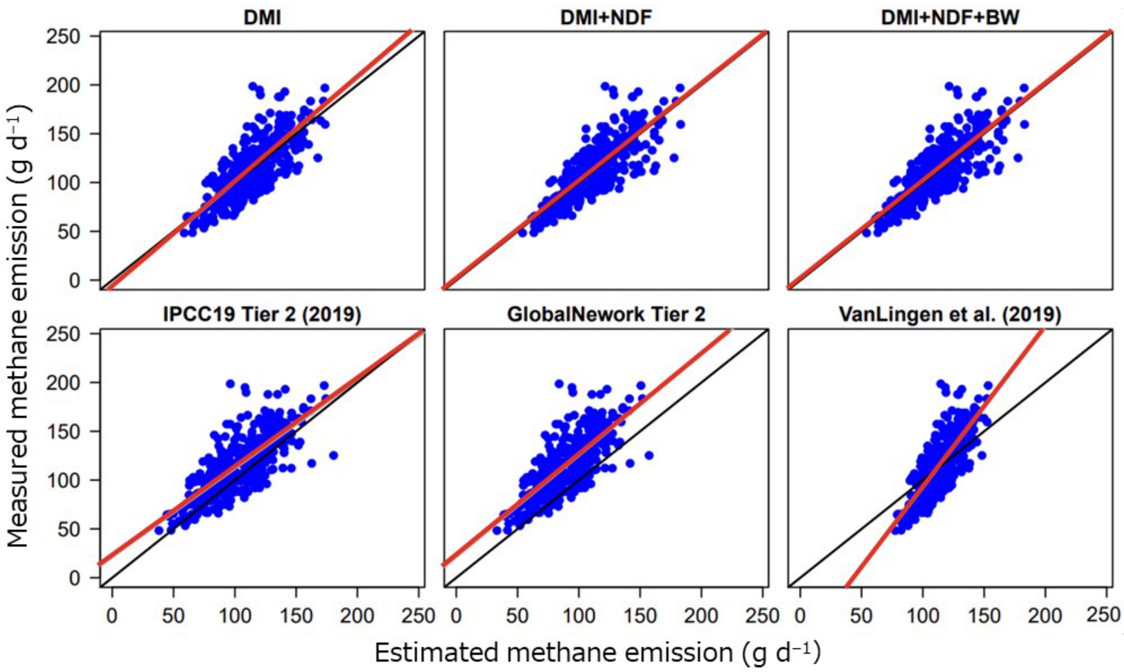

Fig. 1. Observed vs. predicted plots for methane emission (g d^{-1}animal^{-1}) prediction equations

Reference: Tee et al. (2022) *Anim. Feed Sci. Technol.* 294: 115474.
Figures and tables reprinted/modified with permission.

Year-round implementation of alternate wetting and drying across three cropping seasons improves farmers' benefits and reduces greenhouse gas emissions

The Mekong Delta, located in southern Vietnam, is the country's largest paddy rice cropping region. Recently, the area planted with rice has been expanding due to the cultivation of three-season crops. Increasing rice acreage is an effective means of meeting food demand and maintaining or improving farmers' incomes. However, intensive rice cropping system is increasing water demand and greenhouse gas (GHG) emissions.

In rice paddies, the soil becomes anaerobic (without oxygen) and the anaerobic microorganisms produce methane (CH_4), which exacerbates climate change. An irrigation technique called alternate wetting and drying (AWD) is one of the promising technologies that have been developed to reduce irrigation water consumption. This technique supplies oxygen to the soil and reduces CH_4 emissions.

Based on the MeaDRI Strategy and the Global Methane Pledge, JIRCAS is carrying out research about the impact of AWD in the Asia-Monsoon region to facilitate further dissemination. A comprehensive evaluation on the impact of AWD on farmer benefits and GHG emissions, and the merits of year-round implementation across three cropping seasons, has not been done. Therefore, the main objective of this study is to evaluate the impact of year-round AWD implementation on life cycle greenhouse gas (LC-GHG) emissions and farmers' benefits using survey data in 2019-2020 from An Giang Province in the Mekong Delta region of Vietnam. Using the life cycle assessment method, LC-GHG emissions were calculated by summing up emissions from agricultural material production, rice cultivation, harvesting, and rice straw management (Fig. 2).

The results of this study showed that farmers who implemented AWD for three cropping seasons increased their annual financial benefits by 6% compared to farmers who did not implement AWD (Fig. 3). It also revealed that farmers who implement AWD could reduce annual LC-GHG emissions by 38% for the entire year (Fig. 4). Based on these results, this study recommends implementing AWD throughout the year in An Giang Province if irrigation and drainage systems are available.

The implementation of year-round AWD is a co-benefit agricultural system that both increases farmers' benefits and reduces environmental impacts from agriculture, and is expected to be a promising mitigation and adaptation measure for climate change in the Asia-Monsoon region. The results obtained in this study can be used as supporting data for the effectiveness of year-round AWD implementation.

(A. Leon, T. Izumi)

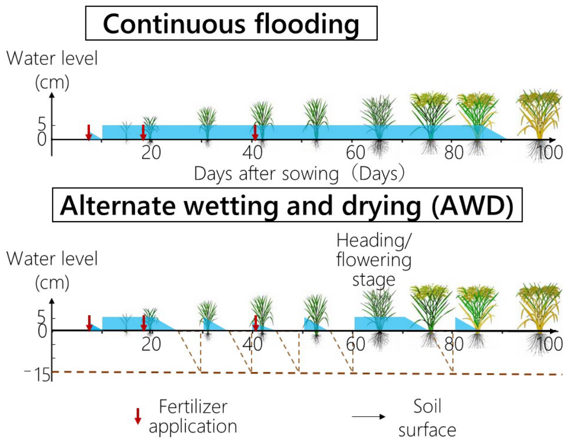

Fig. 1. An example of conventional water management (continuous flooding) and alternate wetting and drying (AWD) during a cropping season

Under AWD, the paddy soil is reflooded to a depth of 5 cm after several days of drying when the water table reaches approximately 15 cm below the soil surface, except for ten days from 10 to 20 days after seeding and during the fertilizer application period and flowering period.

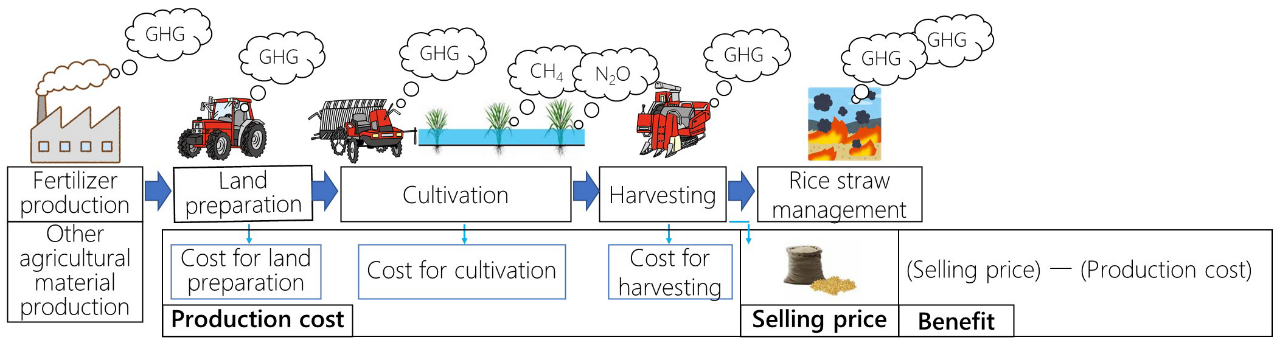

Fig. 2. Life cycle greenhouse gas (LC-GHG) emissions and benefits

LC-GHG is the sum of emissions from agricultural material production to harvesting/rice straw management.

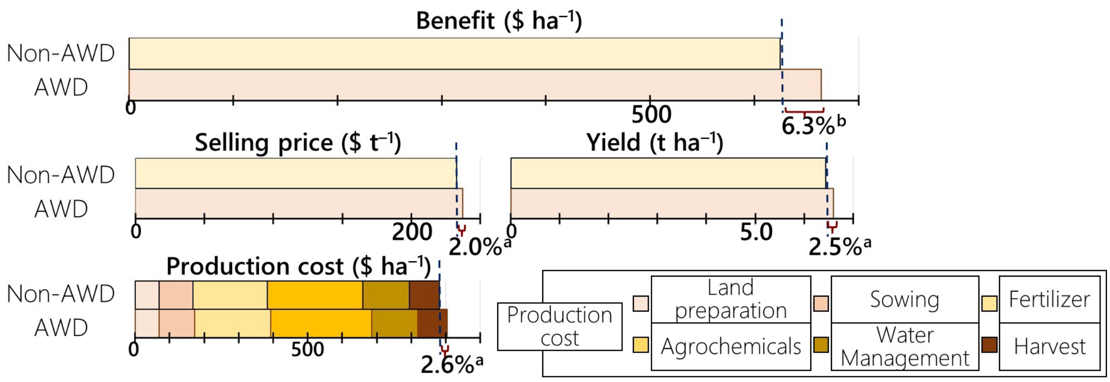

Fig. 3. Benefit, selling price, yield and production cost of non-AWD and AWD farmers

a: $p<0.05$, b: $p<0.056$; n: Number of fields analyzed (501 non-AWD farmers, 535 AWD farmers)

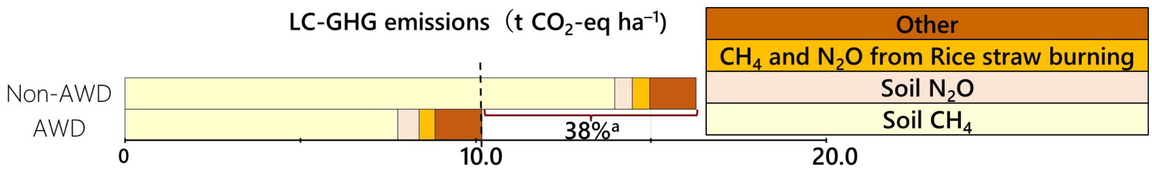

Fig. 4. Life cycle greenhouse gas (LC-GHG) emissions of non-AWD and AWD farmers

a: $p<0.05$; n: Number of fields analyzed (470 non-AWD farmers, 515 AWD farmers)

Reference: Leon and Izumi (2022) *Journal of Cleaner Production* 354: 131621.

Figures modified with permission.

Game theory predicts changes in community values regarding resource allocation held by Subaks in Bali

In the irrigation sector, Water Users Associations (WUAs) play an essential role in ensuring sustainable and efficient resource use while adapting to changes such as climate change and a declining agricultural population. To effectively involve WUAs in sustainable resource management, it is important to lay out the rules in use and the community values of resource use in WUAs, as well as understand the structure of water conflicts. *Subaks*, the traditional WUAs in Bali, Indonesia, are known for their cooperative water management. However, as social structures in Bali are changing, harvesting labor resources are also declining, affecting the water management of subak systems. Using a subak system as a case study, this study proposes a method for analyzing resource allocation conflicts using agent-based modeling and the noncooperative game theory.

An agent-based model was developed to replicate the water allocation system of the target area. In the model, agents representing WUAs with various attributes attempt to maximize annual rice production by following the rules of resource use (Fig. 1). The model's inputs are water and harvesting labor resources, and its outputs are a cropping schedule, seasonal yields, and the annual production of each agent. To assess the strategy combinations of the agents regarding the order of harvesting labor allocation, the noncooperative game was formulated. The strategies of the agents are the cooperative strategy (Cs) and the noncooperative strategy (Ns). If an agent chooses Cs, it prioritizes upstream agents, whereas if it chooses Ns, it prioritizes agents with larger paddy fields. The agents are categorized into 2 players: the upstream and the downstream players, and the total annual productions of the 2 players were examined using a 2 × 2 payoff matrix. To analyze the influence of harvesting labor shortage, three scenarios of different harvesting labor were generated: sufficient, limited, and scarce scenarios. In the sufficient scenario, the total annual production of the downstream player was higher when it chose Ns, contrary to its status quo strategy combination, i.e., when both players chose Cs. This suggests that maintaining cooperative relationships between subaks is outweighed by maximizing individual production (Fig. 2). The results of the limited and the scarce scenarios suggest that as harvesting labor shortage progresses, the value of noncooperative labor resource use increases (Fig. 3), which could affect any allocation of other limited resources.

The results show that the model is useful for analyzing resource allocation conflicts. Additionally, it can potentially evaluate, for example, a countermeasure against harvesting labor shortage before its implementation. As a support tool, this model can help revise resource use rules to adapt to environmental and social changes.

(F. Okura, I. W. Budiasa [Udayana University],
T. Kato [Tokyo University of Agriculture and Technology])

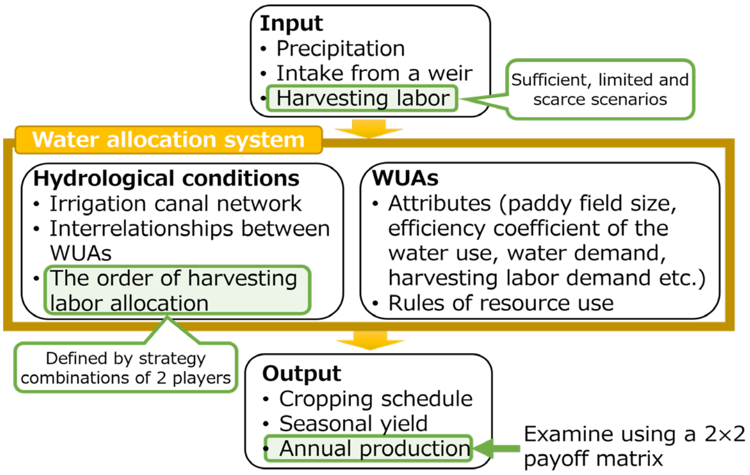

Fig. 1. The model outline
The water allocation system is developed using an agent-based model. Green boxes indicate relation to the application of the noncooperative game theory.

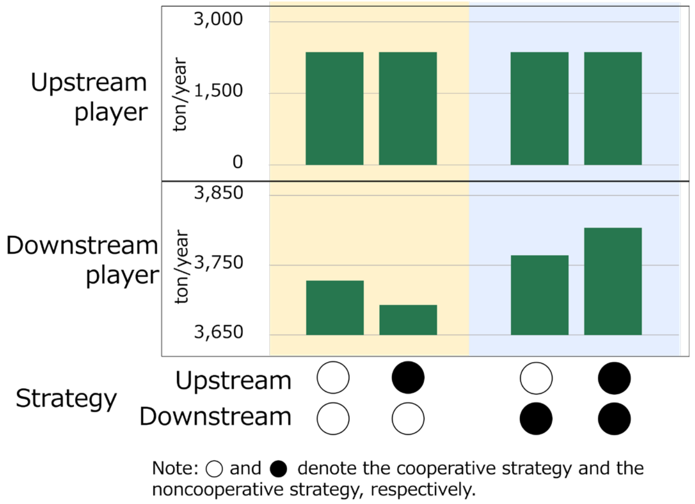

Fig. 2. The total annual production in the sufficient scenario
In the sufficient scenario, the total annual production of the upstream player was the same in any strategy combinations, whereas that of the downstream player was higher when the player chose the noncooperative strategy.

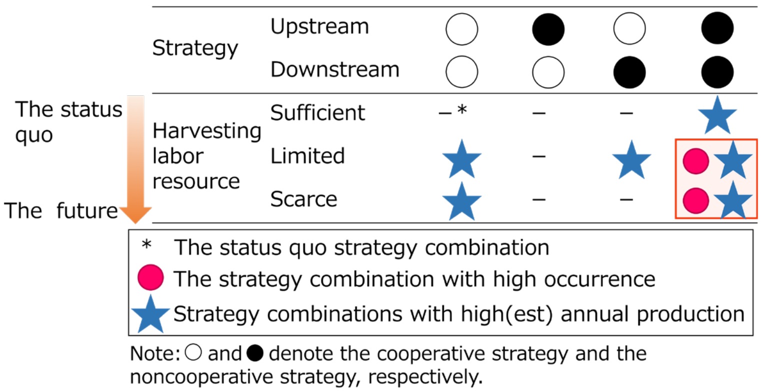

Fig. 3. Results of the noncooperative game in the three scenarios
In the limited and the scarce scenarios, when both the upstream and the downstream players had the noncooperative strategy, the strategy combination became Pareto-optimal and reached the Nash equilibrium.

Reference: Okura et al. (2022) *Agricultural Water Management* 274: 107951.
Figures reprinted/modified with permission.

Technology development to saccharify cellulose “only by cultivating microorganisms" without using cellulase enzymes

Cellulosic biomass, such as fiber and wastepaper discarded from our daily lives, is difficult to decompose in nature, and greenhouse gas emissions from the disposal and incineration of such cellulosic biomass are estimated to exceed 300 million metric tons worldwide. On the other hand, cellulosic biomass is the most abundant resource on earth, hence its effective utilization is required. Until now, its decomposition and saccharification have required large amounts of cellulase enzymes produced by fungi. However, cellulase enzymes are difficult to recycle and expensive to purchase, so there has been a need to reduce the cost of cellulase enzymes.

This report introduces the development of "microbial saccharification," an innovative saccharification technology that can produce glucose directly from cellulose using only microbial cultivation, by co-culturing the thermophilic anaerobic cellulolytic bacterium *Clostridium thermocellum* (hereinafter referred to as "cellulolytic bacteria") with bacteria that produce β-glucosidase, an enzyme that hydrolyzes cellobiose, the result of cellulose saccharification.

By screening with exelin, an artificial substrate, thermophilic anaerobic *Thermobrachium celere* A9 bacteria (NITE P-03454) (hereafter "A9"), which produce "β-glucosidase" outside the bacteria, are isolated from sewage sludge (Fig. 1). Cellulolytic bacteria use the cellobiose produced by cellulose saccharification, and since there is no β-glucosidase activity outside the bacteria, the cellobiose remains in the culture medium as cellobiose. On the other hand, the newly identified A9 cannot saccharify cellulose (Fig. 2A △ and ▲). A9 is a very rare bacterium that produces a potent extracellular β-glucosidase (Fig. 2A ○). The β-glucosidase produced by A9 converts cellobiose into glucose (Fig. 2A ●). As a result, cellulose is degraded with high efficiency, while glucose accumulates in the culture medium (Fig. 2B). This microbial saccharification method is thus an innovative technology that converts cellulose to glucose using only microbial culture without the use of cellulase enzymes.

(A. Kosugi, A. Uke)

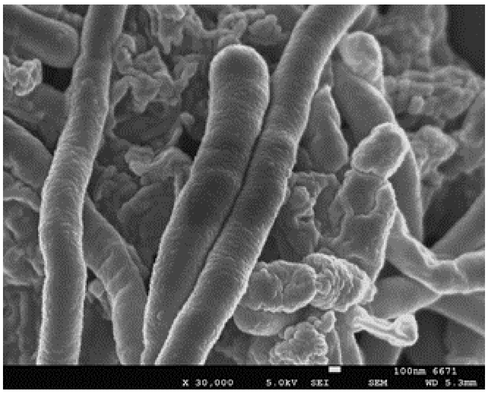

Fig. 1. Electron micrograph of *Thermobrachium celere* A9, which produces the highly active extracellular β-glucosidase

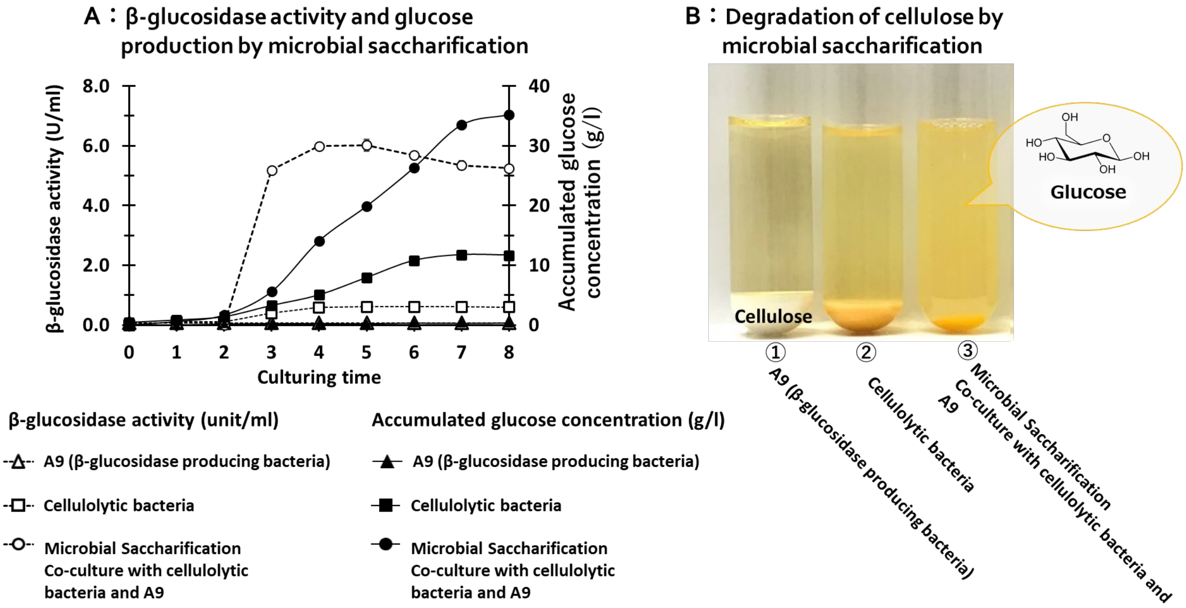

Fig. 2. Glucose production from cellulose by "microbial saccharification" (A) and cellulose saccharification (B)

(A) A9 cannot saccharify cellulose (▲ and △; △ overlaps ▲). The cellulolytic bacteria (□) can degrade cellulose, but produce only a small amount of glucose (■).

On the other hand, in the co-culture of cellulose-poor bacteria and A9 (microbial saccharification method), cellobiose produced by cellulose saccharification is converted to glucose by the extracellular β-glucosidase of A9 bacteria (○) (●).

(B) Accumulation of glucose by the microbial saccharification method (③).

Reference: Nhim, et al. (2022) *Applied Microbiology and Biotechnology* 106: 2133–2145.
Figures reprinted/modified with permission.

Regional population differences in growth characteristics of the Dipterocarpaceae tree species *Shorea leprosula*

Excessive logging has led to the degradation and deforestation of tropical forests dominated by Dipterocarpaceae species in Southeast Asian regions. Furthermore, as the effects of climate change on tropical forests are becoming more apparent, there is an urgent need to establish sustainable afforestation techniques for Dipterocarpaceae species. One of the Dipterocarpaceae species, *Shorea leprosula*, is widely distributed in Peninsular Malaysia and is considered to be one of the most important timber species. On the other hand, there is a concern about an increasing risk of scale insect infestation due to climate change, and the collection of detailed data is becoming urgently important.

Therefore, this study aims to detect differences in growth characteristics among genetically distinct populations and to evaluate tolerance against scale insect infestation in a common garden experiment using *S. leprosula* seedlings from different forest reserves in the Malay Peninsula.

A common garden was established at the Forest Research Institute Malaysia (FRIM) to elucidate the genetic basis of the complex quantitative traits of dipterocarp through genome-wide association studies (Fig. 1A). In this common garden, *S. leprosula* seedlings (Fig. 1B) from nine populations were grown in 40 replications using the random block design (Fig. 1C). We found that the relative growth rate of tree height was highest in population P7 and significantly different from populations P2, P4, and P9 (Fig. 2, $p < 0.05$) and insignificantly different from P1, P3, P5, P6, and P8 ($p > 0.05$). Also, the number of scale insects (*Pedroniopsis* sp.) was the lowest in P7, with significant differences ($p < 0.05$) from P3 and P9 and insignificant from P1, P2, P4, P5, P6, and P8 ($p < 0.05$) (Fig. 3A). In the future, the common garden is expected to be used as a platform for genome-wide association studies, and it will be necessary to investigate the correspondence between genetic differences and phenotypes at the individual level of *S. leprosula*.

(R. Suwa,
C.H. Ng [Forest Research Institute Malaysia (FRIM)], K.K.S. Ng [FRIM], S.L. Lee [FRIM],
C.T. Lee [FRIM], L.H. Tnah [FRIM])

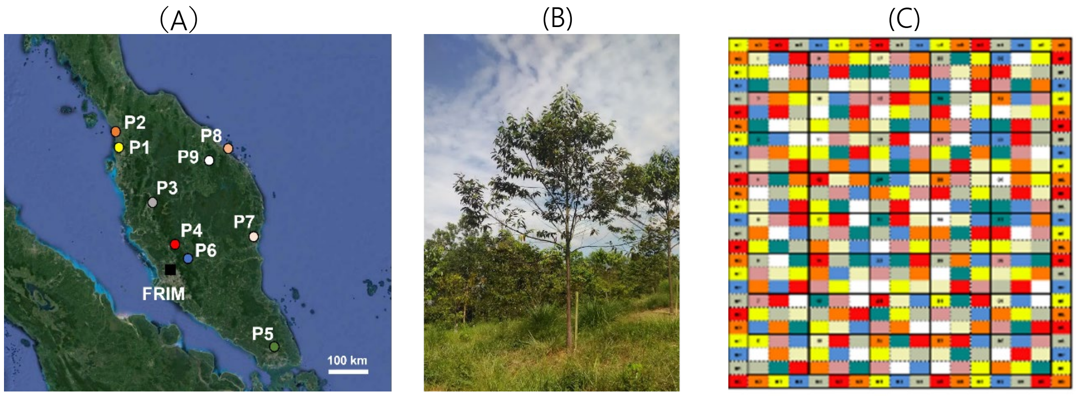

Fig. 1. (A) Sampling sites of seedlings in the Malay Peninsula and Forest Research Institute Malaysia (FRIM), (B) *S. leprosula* planted in the common garden, and (C) the random block design in the common garden

(A) The circles indicate the sampling sites, and the square indicates the location of FRIM where the common garden was established. The numbers indicate the population ID of each sampling site. (B) *S. leprosula* individuals 3 years after planting.
(C) Different colors indicate different populations of the planted seedlings.

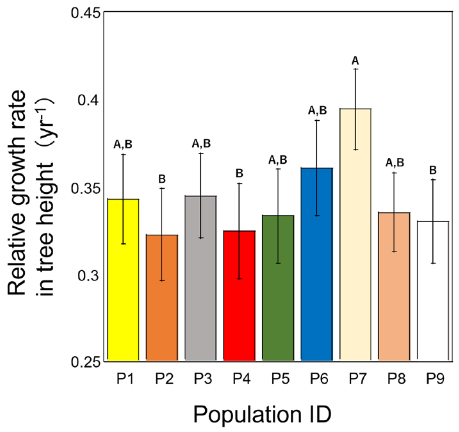

Fig. 2. Relative growth rate of tree height by population

Different letters indicate significant differences (p < 0.05).

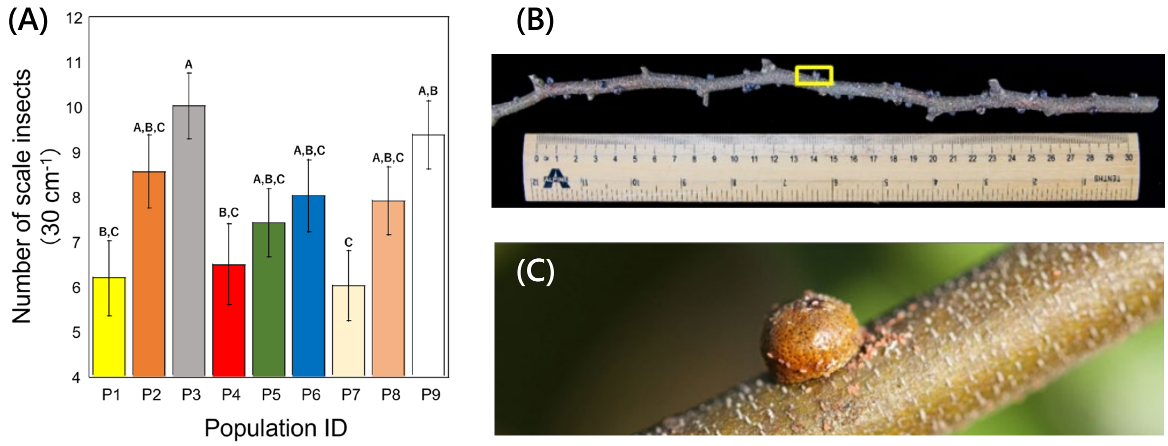

Fig. 3. (A) Number of scale insects on branches in each population, (B) a branch with scale insects, and (C) an enlarged view of a scale insect

(A) Three 30-cm branches were sampled for each individual. The number of scale insects was counted, and the average value is shown. (B) A branch with scale insects, where the yellow box indicates the location of a scale insect (*Pedroniopsis* sp.).

Reference: Ng et al. (2022) *Journal of Forestry Research*. https://doi.org/10.1007/s11676-022-01510-4

Vein structure is related to leaf toughness and photosynthetic capacity in tropical forest trees

Tropical rainforests in Southeast Asia absorb carbon dioxide through high photosynthetic activity and are essential for mitigating climate change. However, they have been degraded by excessive logging, and thus there is a need to restore forest resources through tree planting. In order to ensure successful planting, it is necessary to select tree species suitable for planting environment of the degraded forest through understanding of tree ecological traits such as stress tolerance.

To understand tree ecological traits, we focus on leaf vein structure, which is easy to observe, and develop a method to easily identify tree traits based on leaf morphology in Malaysian tropical rainforest. Tree leaves can be classified into two types of vein structure: leaves with a clearly visible vein network are called heterobaric leaf, while leaves with an indistinct vein network are called homobaric leaf. The former has a transparent fibrous tissue around the veins, which allows light to penetrate, while the latter lacks this tissue (Fig. 1). Leaf toughness and photosynthesis increase with height regardless of species and are related to vein structure (Fig. 2). In taller and brighter environments, heterobaric leaves are more robust and have high photosynthetic ability compared with homobaric leaves. Taller tree species have a higher proportion of heterobaric leaves, while shrubby species tend to have homobaric leaves. Heterobaric leaves are stronger due to their fibrous tissue and higher photosynthesis making them advantageous in environments where leaf defense is required. Homobaric leaves, on the other hand, have much amount of photosynthetic cells instead of fibrous tissue, which allows them to utilize weak light more efficiently, thus favoring photosynthesis in dark environments.

Overall, the leaf vein structure can be used as a convenient indicator for selecting herbivore-tolerant and shade-tolerant tree species from diverse tropical rainforest species. However, it should be noted that a tree's ability to adapt to its environment is not determined solely by the vein structure. For example, tolerance to cold and drought is likely to be related to other traits such as wood density, and thus it is necessary to improve the indicator such as combination with vein structure.

(K. Tanaka,
T. Ichie [Kochi University], M. Mohizah [Forest Department Sarawak])

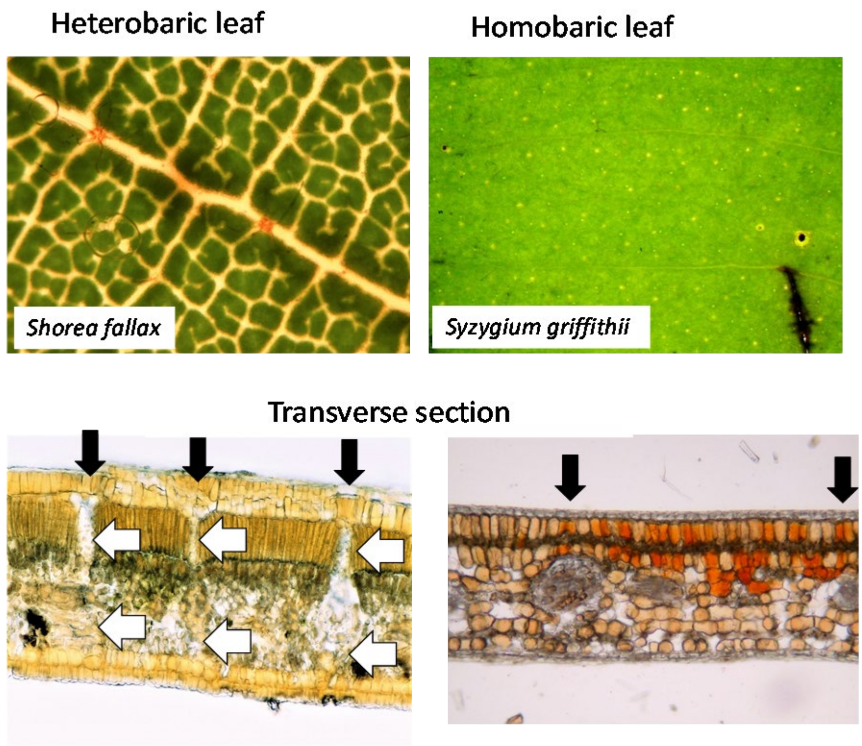

Fig. 1. Different structure of veins between heterobaric and homobaric leaves

Tree leaves can be divided into two groups: those with clear veins when exposed to light (heterobaric leaf, left) and those with indistinct veins (homobaric leaf, right). Heterobaric leaves have bundle sheath extensions (white arrows) by fibrous tissue around vascular bundles (black arrows).

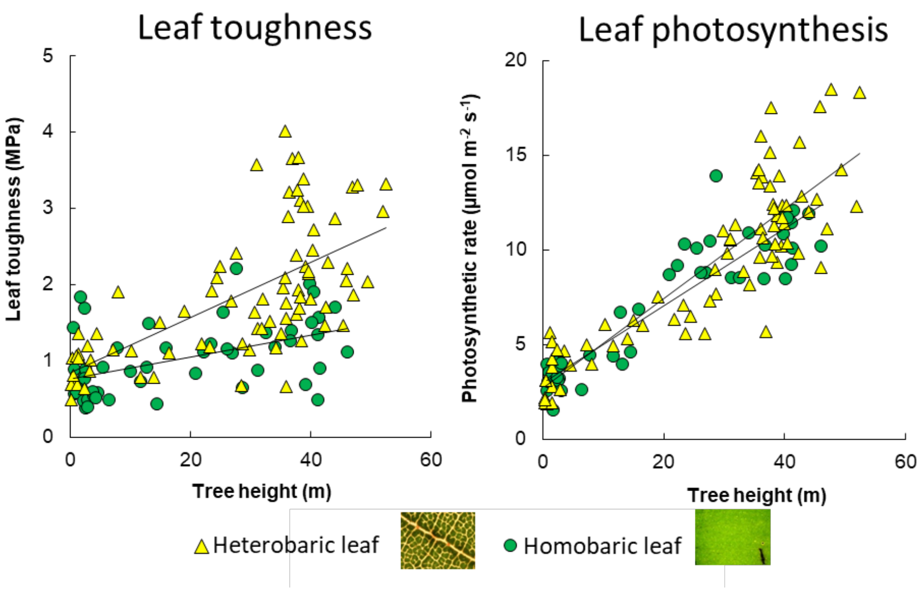

Fig. 2. Variation in leaf toughness (left) and photosynthesis (right) with tree height

Leaf toughness and photosynthesis increase with tree height. In tall trees (around 40 m), which are exposed to strong light and strong winds, heterobaric leaf species tend to have more robust leaves and higher photosynthesis than homobaric leaf species.

Reference: Kenzo et al. (2022) *Frontiers Forest Global Change* 5: 1002472.

Intergeneric hybrid between sugarcane and *Erianthus* exhibits superior nitrogen use efficiency than sugarcane

Nitrate-nitrogen leaching from farmland has adverse effects on drinking water and environmental conservation in tropical and subtropical island regions such as the Southwest Islands of Japan. Sugarcane is widely grown in these areas, and it is necessary to increase the nitrogen use efficiency of this crop to reduce nitrogen leaching. Studies on nitrogen utilization in this species have focused on yield potential and fertilizer management; however, there have been only a few breeding attempts. The relationship between root system characteristics and nitrogen utilization is also unclear, while improvement of nitrogen utilization using *Erianthus arundinaceus* can be expected because of its unique root system characteristics. In the present study, nitrogen leaching and root system characteristics of sugarcane × *Erianthus* intergeneric hybrid and parental genotypes were investigated using a lysimeter to verify the possibility of improving nitrogen utilization characteristics.

Nitrogen leaching was significantly lower under the parental *Erianthus* from the early growth stage, while it was significantly lower in the intergeneric hybrid in the mid-growth stage than that in the parental sugarcane. The nitrogen use efficiencies of *Erianthus* and the intergeneric hybrid were significantly greater than that of sugarcane. *Erianthus* and the intergeneric hybrid exhibited lower shoot/root ratio and deeper rooting than sugarcane and consumed significant amounts of soil moisture in the deeper layers, suggesting that root mass and deeper rooting may be factors in reducing nitrogen leaching. These results indicate the possibility of improving the nitrogen utilization characteristics of sugarcane by improving its root system characteristics using *Erianthus*.

The intergeneric hybrid F_1 can be used to breed sugarcane varieties that contribute to reductions of nitrogen leaching and fertilization. However, it is necessary to improve the sugar content of the F_1 line through backcrossing with sugarcane varieties in order to utilize it as a variety for sugar production because the F_1 line has low sugar content at harvest season. In addition to root elongation characteristics, nitrate preference may also be related to greater nitrogen use efficiency, which should be investigated in future studies using the N^{15} tracer method.

(H. Takaragawa, K. Okamoto, Y. Terajima, T. Anzai)

Fig. 1. Outline of lysimeter study

Sugarcane (NiF8), *Erianthus* (JIRCAS1), and intergeneric hybrid F_1 (J08-12) were grown under lysimeter conditions (n=4 plots) from Sept. 2020 to May 2021.

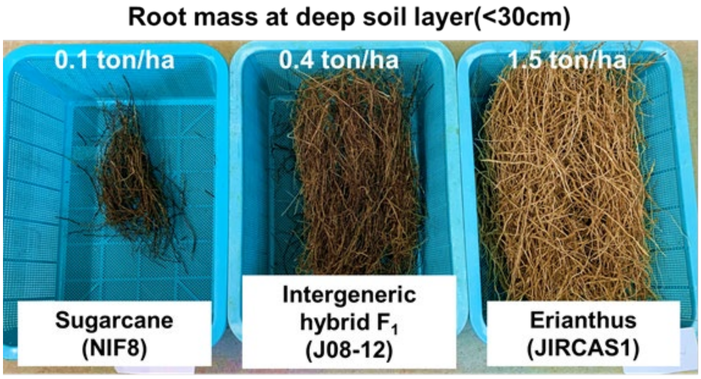

Fig. 2. Root mass of each genotype

Values indicate root mass at deep soil layer with significant genotypic differences.

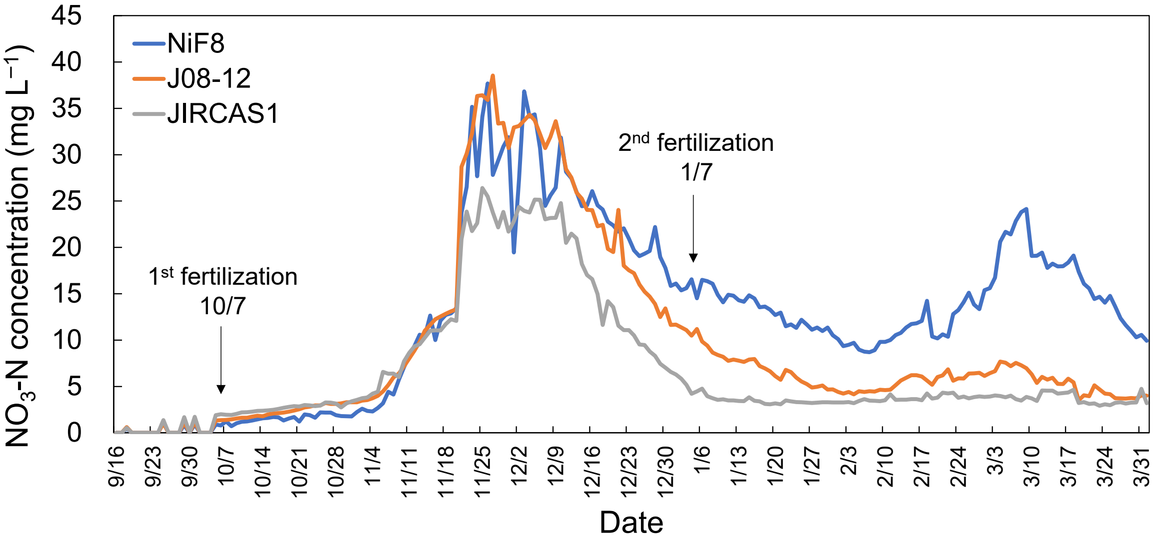

Fig. 3. Changes in nitrate-nitrogen concentration in drainage water during the growth period

Survey was conducted from September 2020 to March 2021. Arrows indicate fertilization dates.

Table 1. Characteristics of nitrogen use and biomass partition

Genotype	Drainage NO^3-N (kg ha^{-1})	Total dry mass (ton ha^{-1})	Shoot mass/ Root mass ratio	Root depth index (cm)	Total N uptake (kg ha^{-1})	N use efficiency (g gN^{-1})
Sugarcane (NiF8)	42.6 b	17.0 a	30.7 c	24.8 a	104.5 a	163.5 a
Intergeneric hybrid F_1 (J08-12)	32.4 b	27.6 b	24.8 b	31.6 b	136.3 b	202.4 b
Erianthus (JIRCAS1)	17.8 a	26.4 b	6.4 a	35.7 b	128.3 ab	206.7 b

Higher root depth index indicates deeper root system. Nitrogen use efficiency is calculated by dividing total biomass by total nitrogen uptake. Different alphabet means significant differences among genotypes at $P < 0.05$ (Tukey, n=4).

Reference: Takaragawa et al. (2022) *Plant Production Science* 25: 298–310.

Predicting riverine nutrient concentrations from catchment characteristics using a machine learning method

Excessive loadings of terrestrial nitrogen and phosphorus, and their imbalances with silicon have been recognized as one of the major causes of water quality and ecosystem deterioration in receiving coastal waters around tropical islands. In this study, water quality was monitored every two months for one year in the rivers and streams of Ishigaki Island, a tropical island in Japan (Fig. 1), to analyze how the catchment characteristics (e.g., land use, geology) influence the concentrations of dissolved inorganic nitrogen (DIN), total phosphorus (TP) and dissolved silicon (DSi).

Based on the monitoring results, predictive models for nutrient concentrations from the catchment properties were created using Random Forest (RF) machine learning algorithm. Coefficient of determination (R^2) between the observed and predicted values were 0.87 ~ 0.96 and 0.69 ~ 0.88 for training and testing data sets, respectively, and the percent bias (PBIAS) were –0.33 ~ 0.36% and –1.30 ~ 0.06%, demonstrating that the created models can predict nutrient concentrations with sufficient accuracy (Fig. 2). Contributions of the catchment properties to nutrient concentrations can be also evaluated from their importance in the RF models in combination with the correlation coefficients with nutrient concentrations. Agricultural land uses (e.g., livestock barn, sugarcane field) were ranked as the most important parameters in the RF models for DIN and TP, and they also had strong positive correlations (Spearman's rank correlation coefficients being more than 0.7) with these nutrients (Fig. 3). Considering that fact that sugarcane cultivation and beef calf raising are active in Ishigaki Island, these results suggest that these agricultural activities have strong influences on riverine nitrogen and phosphorus concentrations. On the other hand, forest was not only the most important parameter in the RF model for DSi but also strongly positively correlated with DSi concentration (Fig. 3), suggesting that forest serves as a dominant source of riverine Si.

As the RF models can be operated in a relatively easy way, they can be utilized for formulating action plans toward conservation of coastal water quality and ecosystems (e.g., identification of rivers that need to be monitored with respect to nutrient loading to coastal water). These models would also be applicable for predicting the variations in riverine nutrient concentrations due to the change in catchment land use and management, while the predictions need to be validated through the comparison with those of process-based hydrologic models.

(T. Kikuchi, T. Anzai)

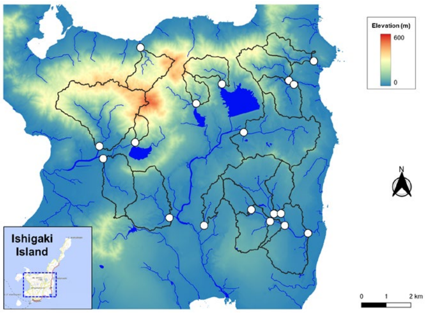

Fig. 1. Study site (left); river water sampling (right)
White circles and black lines in the left panel represent the sampling stations and catchment boundaries, respectively.

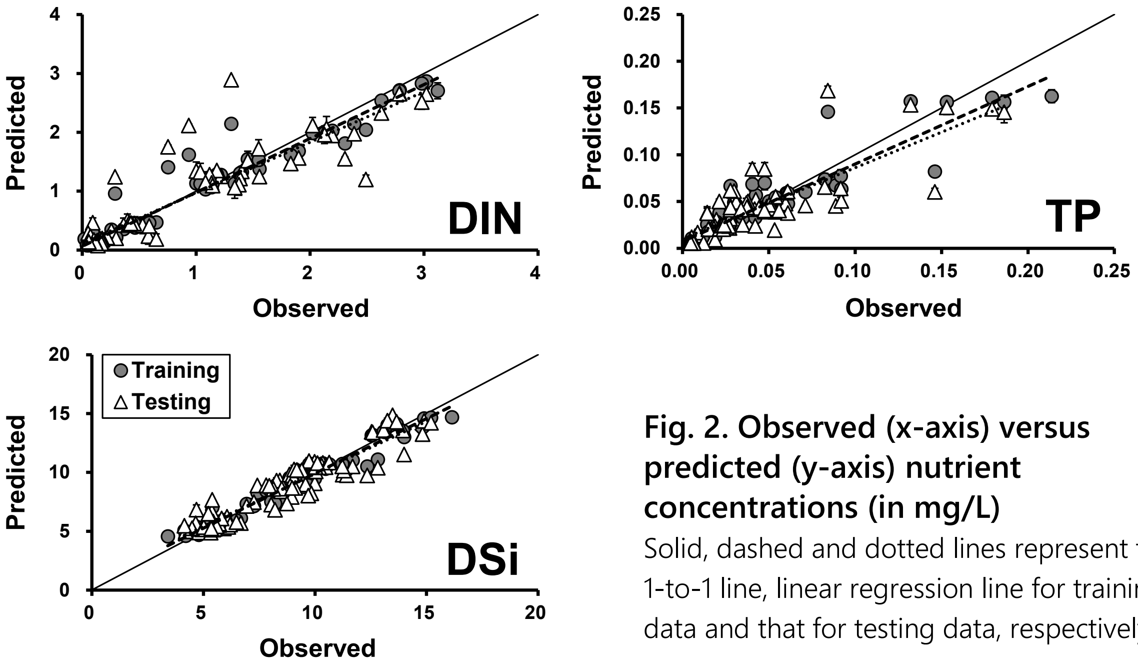

Fig. 2. Observed (x-axis) versus predicted (y-axis) nutrient concentrations (in mg/L)
Solid, dashed and dotted lines represent the 1-to-1 line, linear regression line for training data and that for testing data, respectively.

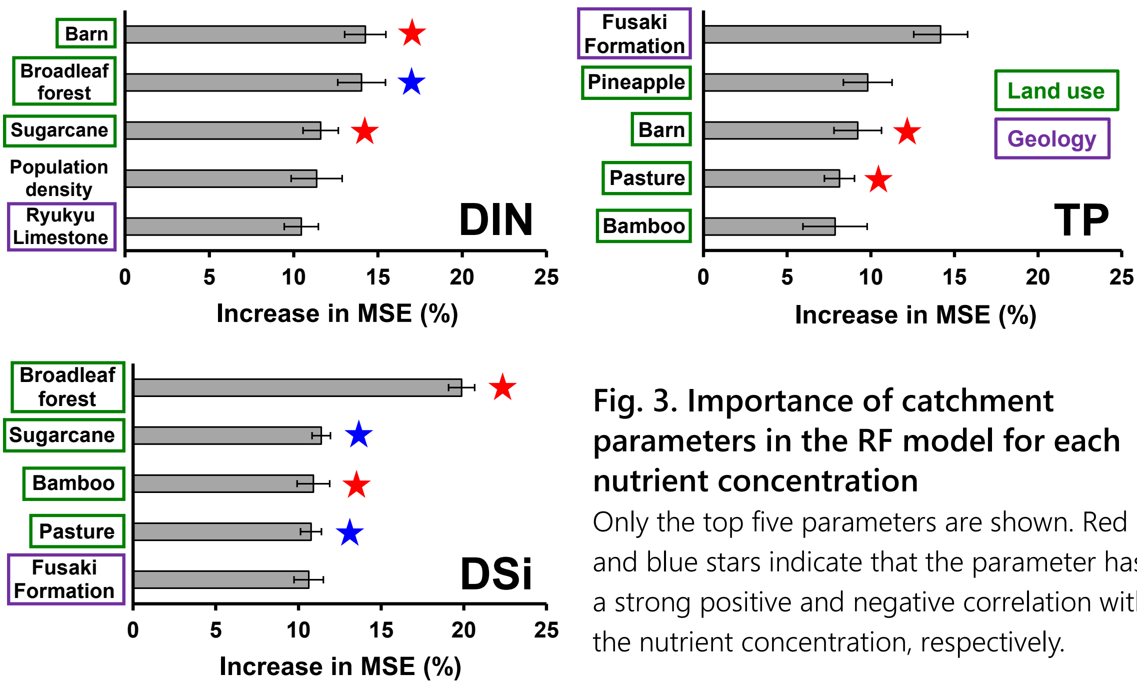

Fig. 3. Importance of catchment parameters in the RF model for each nutrient concentration
Only the top five parameters are shown. Red and blue stars indicate that the parameter has a strong positive and negative correlation with the nutrient concentration, respectively.

Reference: Kikuchi et al. (2023) *Environmental Pollution* 316: 120599.

Shallow sub-surface drainage constructed with "Cut-soiler" mitigates soil salinity

In the Indo-Gangetic Plain, groundwater irrigation dramatically improved agricultural production. However, salinization has become a serious issue due to the high salinity of irrigation water and poor drainage. Construction of open and/or sub-surface drainage is effective at mitigating salinization, but it is difficult for farmers to implement due to the high cost. Therefore, towards developing sustainable drainage measures that farmers can practice, we conducted research and created a low-cost method of constructing shallow sub-surface drainage using a Japan-built tractor attachment called the "Cut-soiler."

Conventionally, when constructing a material-filled sub-surface drainage, it is necessary to prepare the hydrophobic material to be buried in the soil and load it into the construction machine. This method does not require these works, and harvested residues such as rice and wheat straw scattered on the field can be buried underground simply by running a tractor equipped with the Cut-soiler. The method involves cutting the soil into an inverted trapezoid, then lifting it up to make space from the ground surface to a depth of 40 to 60 cm. The crop residue, spread to a width of 120 cm, is then pushed into this space to make a shallow sub-surface drainage (Fig. 1). Shallow sub-surface drainage (60-cm depth) constructed with the Cut-soiler reduced soil salinity (ECe: electrical conductivity of the solution extracted from the saturated soil) by 8% (no significant difference) and 32% (P=0.047) at 4 and 16 months after construction, respectively (Fig. 2). Meanwhile, the yield improved by 4% (no significant difference) and 23% (P=0.048) in the dry season crop (November to March: mustard) and in the rainy season crop (June to September: pearl millet), respectively (Fig. 3).

The construction method has been compiled into a manual, titled "Cut-soiler constructed Preferential Shallow sub-surface drainage for mitigating salinization User's Guide," and is now available on the JIRCAS website for its further extension. It is expected to be used for salinization countermeasures by the Central Saline Soil Research Institute (CSSRI) in India. Regarding the method and equipment, the following should be noted. The drainage condition should be checked in advance as this method depends on the drainage condition around the field. Then, a suitable construction method should be chosen. The Cut-soiler does not have wheels, so it must be loaded onto a truck when transporting long distances. The estimated useful life of the Cut-soiler is around 7 years covering 30–50 ha of construction area per year. If there is no problem with the frame, it can be used continuously by simply replacing consumables.

(J. Onishi, K. Koda, K. Matsui, T. Anzai, K. Okamoto, G. Lee, T. Watanabe, K. Omori, I. Kitagawa [National Agriculture and Food Research Organization], Chaudhari S.K. [Indian Council of Agricultural Research], Yadav R.K. [ICAR-Central Saline Soil Research Institute], Yadav G. [ICAR-CSSRI], Neha [ICAR-CSSRI], Rai A.K. [ICAR-CSSRI], Kumar S. [ICAR-CSSRI], Narjary B. [ICAR-CSSRI], Sharma P.C. [ICAR-CSSRI])

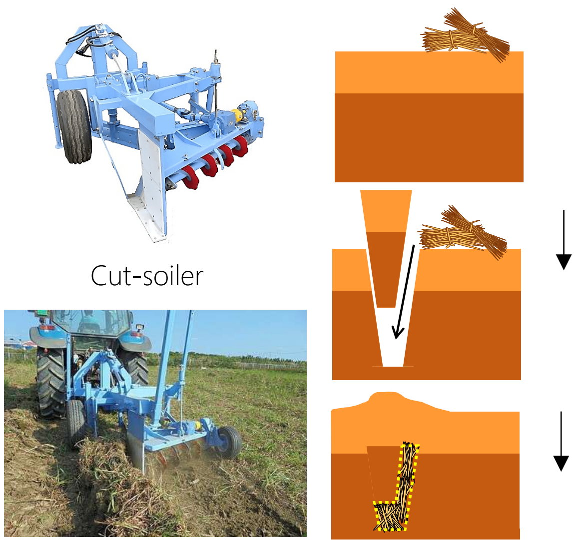

The shredded residue (straw, stems, and leaves) and compost are left on the field after harvesting.

Driven by a tractor, the Cut-soiler cuts the soil into an inverted triangular (V) shape and lifts the soil to open a trench. At the same time, the surface materials are collected and pushed towards the narrow groove formed during trench opening.

The lifted soil is backfilled over the filling material, creating a groove-shaped, shallow sub-surface drainage.

Since the ground is raised after construction, the field should be leveled with a rotary or leveling disc harrow, etc.

Fig. 1. Method of constructing a shallow sub-surface drainage with the Cut-soiler

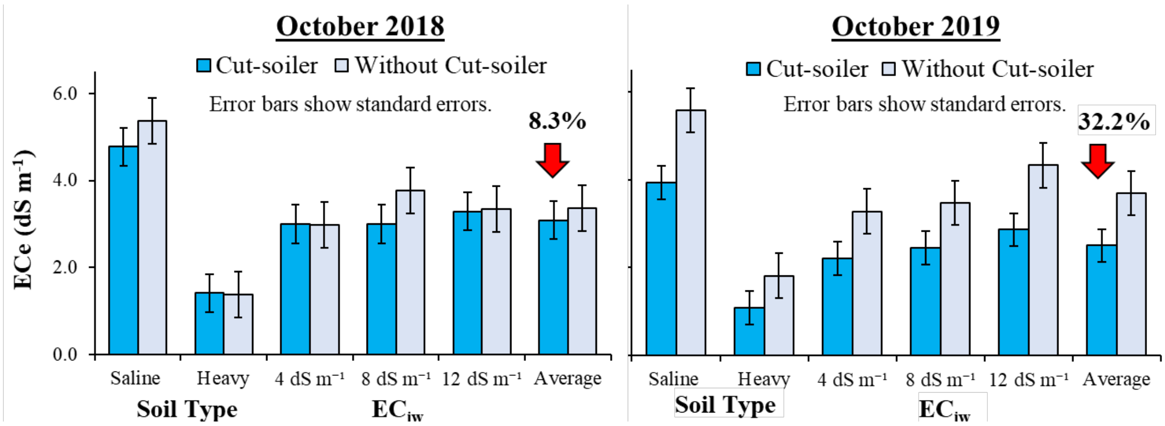

Fig. 2. Changes in soil salinity

EC_{iw} is the electrical conductivity of irrigation water.
Average is the average of 12 plots with and without Cut-soiler construction.

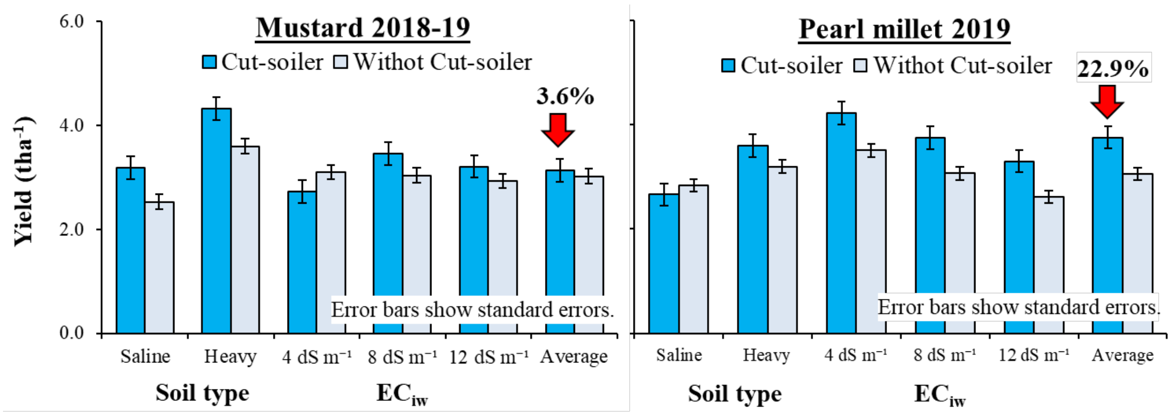

Fig. 3. Yield of dry season crop (mustard) and rainy season crop (pearl millet)

EC_{iw} is the electrical conductivity of irrigation water.
Average is the average of 12 plots with and without Cut-soiler construction.

References: Fig. 1. NARO Research Highlight (2015); Figs. 2 and 3. Neha et al. (2022) *Journal of Arid Land Studies* 32(S): 117–122. https://doi.org/10.14976/jals.32.S_117
Figures reprinted/modified with permission.

Novel genetic loci that elongate rice roots under different nitrogen conditions

To reduce the impact of nitrogen on the environment, it is expected that varieties with improved nitrogen utilization will be developed. One strategy to promote nitrogen utilization (uptake) is to improve the elongation of rice roots and increase the size of the root system. Therefore, identifying the loci involved in rice root length and develop DNA markers for line selection is crucial. The nitrogen available to rice varies with the growing environment. Under reducing waterlogged conditions (irrigated paddy fields), where irrigation water is available, ammonia-form is the main source of nitrogen supply. On the other hand, in rain-fed paddy fields and upland rice cultivation, which are prone to dry conditions and oxidative conditions, nitrate-form nitrogen may be the source of nitrogen supply. Therefore, to estimate the available cultivation conditions, it is necessary to set up experimental conditions in which ammonia-form nitrogen and nitrate-form nitrogen are the sole sources of nitrogen supply.

We set up four hydroponic conditions adjusted to 5 µM or 500 µM of NH_4Cl as ammonia-form nitrogen and KNO_3 as nitrate-form nitrogen. Line YTH187, which contains chromosomal fragments derived from IR69093-41-2-3-2 (YP5) in the genetic background of IR64, has a significantly longer root length than IR64 under all conditions (Figs. 1 and 2). Among the genetic loci that increase root length in YTH187, *qRL4.1-YP5* is located between the molecular markers RM3534 and RM6909 on chromosome 4 and elongates roots only in the 5 µM nitrate-nitrogen condition (Fig. 3). These results suggest that it is effective in a nitrate-nitrogen-specific manner and may be effective in oxidative, low-fertility rainfed and upland rice fields. *qRL8.1-YP5* (R^2=0.09–0.16), located between RM8271 and RM3395 on chromosome 8, elongates roots under growing conditions with 500µM NH_4Cl or KNO_3. This result may be effective in irrigated and rainfed/upland rice cultivation with high nitrogen fertilization levels. *qRL5.3-YP5* (R^2=0.10–0.11) is located between RM1089 and RM4691 on chromosome 5 and elongates roots under all growing conditions. *qRL6.5-YP5* (R^2=0.12–0.22) is located between RM5509 and RM1370 on chromosome 6 and elongates roots under both low- and high-concentration root elongation under both nitrogen conditions. These results suggest that the two loci may be effective under a wide range of growing conditions.

The DNA marker information of *qRL4.1-YP5*, *qRL5.3-YP5*, *qRL6.5-YP5*, and *qRL8.1-YP5* can be used for marker selection to improve the efficiency of nitrogen absorption through root morphology improvement. The effect was observed in the genetic background of IR64, which can contribute to the improvement of Indian-type cultivars grown in many tropical regions. The effects on root mass, nitrogen uptake, and productivity in the field need to be verified by growing near-isogenic lines carrying each locus alone.

(K. Sasaki, M. Obara)

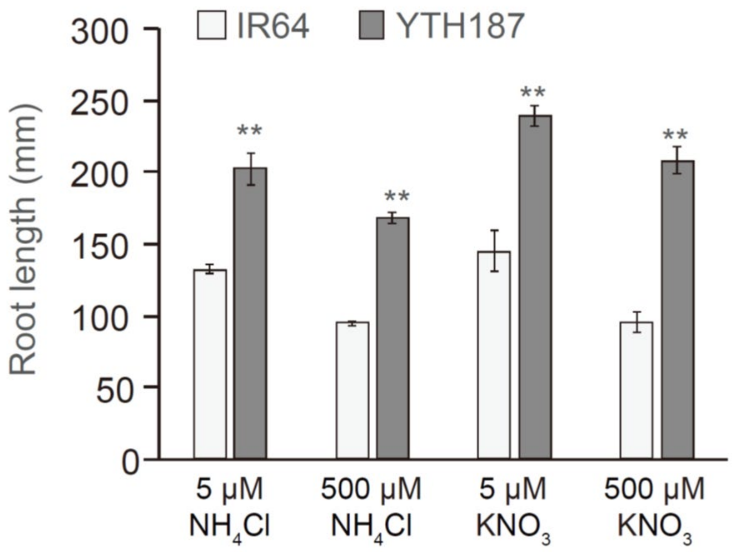

Fig. 1. Root length of YTH187 and IR64 grown for 8 days in each treatment
**: *t*-test indicates significant difference at 1% level (n=4).

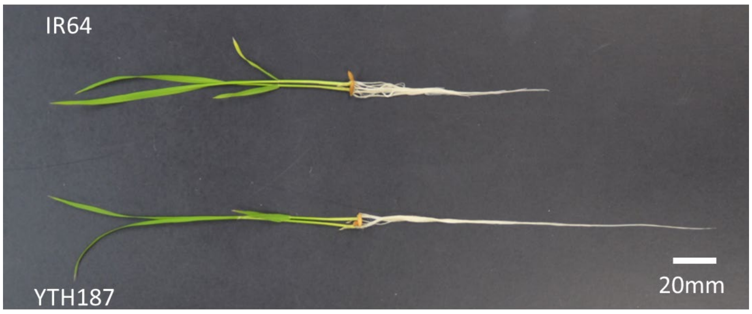

Fig. 2. Root length of YTH187 and IR64 in the presence of 500 μM nitrate nitrogen
IR64 (top) and YTH187 (bottom) grown for 8 days

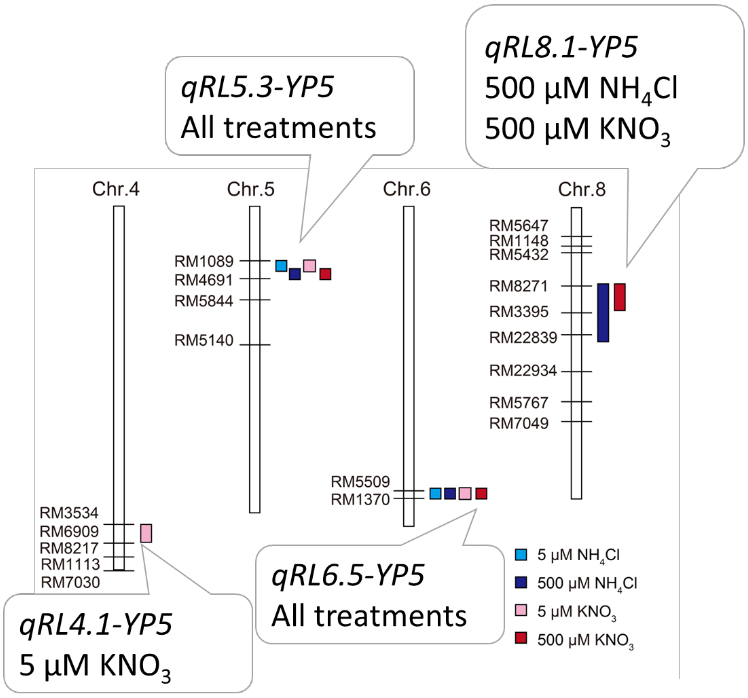

Fig. 3. Location and condition of detected genetic loci
The region where each gene is located and the nitrogen condition under which it was detected. The bar range indicates the locus region.

Reference: Sasaki and Obara (2022) *Soil Science and Plant Nutrition* 68(4): 454–462.
Figures reprinted/modified with permission.

Enlargement of grain size improves nitrogen utilization efficiency in rice

The Green Revolution made it possible to increase crop yields through the application of large amounts of nitrogen (N) fertilizers, but it also resulted in serious environmental pollution. In addition, such production systems are vulnerable to high N fertilizer prices. Therefore, toward sustainable production and supply of rice, increasing the crop grain yield must be achieved without such a considerable input of N fertilization. Our previous studies demonstrated that a large-grain *japonica* rice cultivar, Akita 63, has high nitrogen utilization efficiency per unit of absorbed nitrogen (PNUE) and a large-grain allele of the *GS3* gene. To examine the positive effect of the large-grain allele of *GS3* on rice yields, PNUE, and nitrogen utilization efficiency per unit of fed nitrogen fertilizer (NUE), a near-isogenic line of the large-grain allele of *GS3* originated from Akita 63 was developed in the genetic background of a *japonica* cultivar, Notohikari, with a large grain (LG-Notohikari).

LG-Notohikari always showed longer and wider grains compared to Notohikari in any fertilizer conditions (Fig. 1). Significant grain yield increases for LG-Notohikari were observed in two fertilized plots, with application rates equal to 4.8 and 9.6 g N/m^2, but not observed in the unfertilized plot (Table 1). Among yield components, thousand-grain weight showed significant increases in all conditions tested. Also, grain yield of the LG-Notohikari grown in the 4.8 g N/m^2 plot was similar to that of the Notohikari grown in the 9.6 g N/m^2 plot. NUEs of the LG-Notohikari were significantly higher than those of the Notohikari in both N applications (Fig. 2). Likewise, PNUE of the LG-Notohikari was higher than that of the Notohikari (Fig. 3).

Enlargement of grain size using the large allele of *GS3* improves nitrogen utilization efficiency in rice and can be used in a rice breeding program for reduced amounts of N fertilizer. It should be noted that the effect of improving NUE and grain quality by the enlargement of grain size depends on original varieties, growth conditions, environments, and other factors.

(M. Obara,
Yoon D.K. [Graduate School of Agricultural Science, Tohoku University],
K. Ishiyama [Graduate School of Agricultural Science, Tohoku University],
A. Makino [Graduate School of Agricultural Science, Tohoku University])

Fig. 1. Typical phenotypes of Notohikari and LG-Notohikari grains

Ten grains each of the Notohikari and LG-Notohikari were prepared, and plants were grown in a field in Aobayama, Miyagi, Japan, without N fertilizer application. The scale bar

Table 1. Grain yield and yield components of Notohikari and LG-Notohikari grown with different amounts of N fertilizer

N fertilization	Line	Paddy yield	Total spikelet	Seed fertility	1,000-grain
0	Notohikari	269±4 a	15.0±0.2 a	76.2±1.4 a	24.6±0.5 a
	LG-Notohikari	287±9 a	15.0±0.2 a	74.4±1.8 a	31.0±1.5 b
4.8	Notohikari	338±17 a	21.0±0.6 a	80.3±1.4 a	25.6±0.4 a
	LG-Notohikari	456±26 b	22.0±0.8 a	79.8±1.1 a	29.3±0.6 b
9.6	Notohikari	450±31 a	30.1±0.8 a	76.7±1.4 a	23.1±0.6 a
	LG-Notohikari	535±21 b	28.3±0.8 a	81.8±1.9 a	28.6±0.5 b

Plants were grown at a JIRCAS paddy field in Tsukuba, Ibaraki, Japan. The mean values and standard errors are indicated. Different letters indicate significant differences (P value less than 0.05) between Notohikari and LG-Notohikari in each condition (n=10).

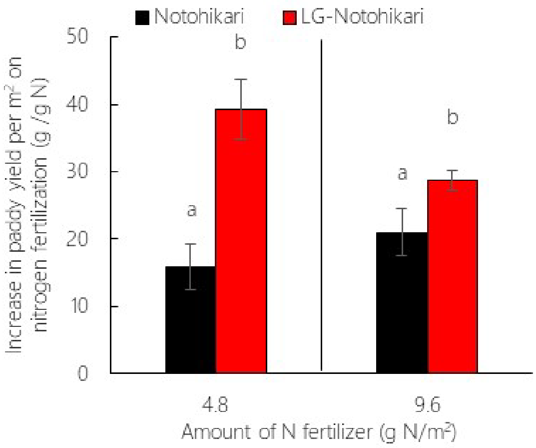

Fig. 2. NUEs of the Notohikari and LG-Notohikari

Plants were grown at a JIRCAS paddy field in Tsukuba, Ibaraki, Japan. The mean values and standard errors are indicated. Different letters indicate significant differences (P value less than 0.05) between Notohikari and LG-Notohikari in each condition (n=10).

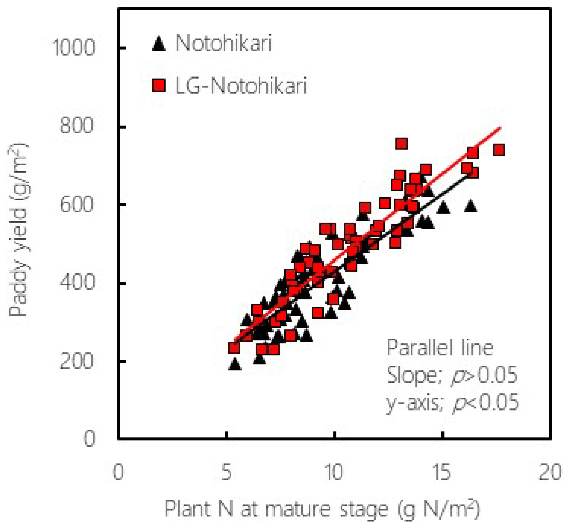

Fig. 3. PNUEs of the Notohikari and LG-Notohikari

Relationship between plant N at mature stage and paddy yield of plants grown at a Kawatabi paddy field in Osaki, Miyagi, Japan

Reference: Yoon et al. (2022) *Plant Direct* 6(7): e417. https://doi.org/10.1002/pld3.417
Figures and table modified with permission.

Development of the new soybean variety "Sudou 27"

Saline soils cover approximately 830 million hectares globally (FAO), with around 53% of this area located in Asia. Salinity problems lead to reduced crop productivity in these regions. Therefore, the development of crop varieties with high salt tolerance is necessary to adapt to saline soils. Previously, we identified the salt-tolerant gene *Ncl* from a Brazilian soybean variety and demonstrated that soybean lines carrying *Ncl* can maintain high seed yields in saline fields. *Ncl* is now being used in soybean breeding practices in China, Vietnam, and India. "Sudou 27," a new soybean variety, was developed in collaboration between the Jiangsu Academy of Agricultural Sciences, China, and the Japan International Research Institute for Agricultural Sciences, Japan.

"Sudou 27" (Fig. 1) was selected from the progenies of a cross between soybean lines 1138-2 and NILs72-T. NILs72-T harbors the salt tolerance gene *Ncl*. Based on three-year field evaluation results, "Sudou 27" was recognized for its excellent traits by the Crop New Variety Inquiry Committee of Jiangsu Province, China, and was registered as a new soybean variety in China on August 29, 2022. "Sudou 27" showed high seed yield and high seed quality characteristics, with a 6.9% higher seed yield (3.14 t/ha) and 1.4% higher seed oil content (22.4%) than the leading soybean cultivar in the northern region of Jiangsu Province, "Xudou 13," which was used as control variety in the new variety test and productivity test experiments (Table 1). In a salt tolerance evaluation test conducted by treating the seedlings with 120 mM NaCl solution for three weeks, "Sudou 27" showed higher salt tolerance than "Xudou 13" (Fig. 2). In addition, "Sudou 27" exhibited moderate resistance to soybean mosaic disease caused by the soybean mosaic virus (SMV) (Table 1).

"Sudou 27" is expected to become one of the leading soybean varieties in the northern area of Jiangsu Province, China, replacing the former leading variety "Xudou 13." The successful development of this new variety using the salt tolerance gene *Ncl* has paved the way for breeding salt-tolerant varieties that are expected to contribute to the sustainability of soybean production in areas with salinity problems.

(D. Xu,
H. Chen [Jiangsu Academy of Agricultural Sciences (JAAS), P.R. China], X. Cui [JAAS],
H. Zhang [JAAS], X. Liu [JAAS], Q. Wang [JAAS], X. Chen [JAAS], H. Gu [JAAS])

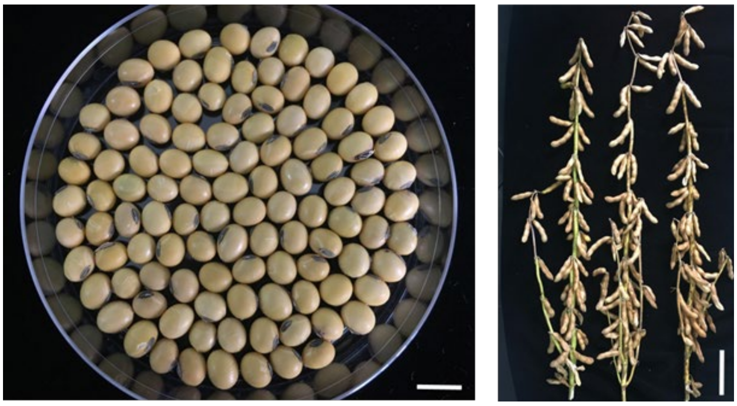

Fig. 1. "Sudou 27" seeds (left, scale bar = 1 cm) and mature plants (right, scale bar = 10 cm)

Table 1. Characteristics of "Sudou 27"

	New variety test experiment [a] (2019～2020, 6 test sites)							Productivity test [b] (2021, 7 test sites)
	Grain yield (t/ha)	Growth period (day)	100-seed weight (g)	Seed quality		Resistance level to SMV [c]		Grain yield (t/ha)
				Oil content (%)	Protein content (%)	Race SC-3	Race SC-7	
Sudou 27	3.27	104.5	17.0	22.4	38.7	Moderate resistance	Moderate resistance	3.14
Xudou 13 [d]	3.14	101.0	25.6	21.0	40.3	Moderate susceptibility	Moderate susceptibility	2.94

[a] New variety test experiment: The experiment was conducted for 2 years at 6 test sites. The plot area for each line (variety) was 9.6 m^2 with 3 replicates. [b] Productivity test: Productivity test was conducted for the new variety candidate lines that passed the new variety test experiment. It was conducted for 1 year at 7 test sites. The plot area for each line (variety) was 150 m^2 with 2 replicates. [c] SMV: Soybean mosaic disease. [d] Xudou 13: A leading soybean cultivar in the northern region of Jiangsu Province, China. It was used as control variety in the new variety test experiment and the productivity test experiment.

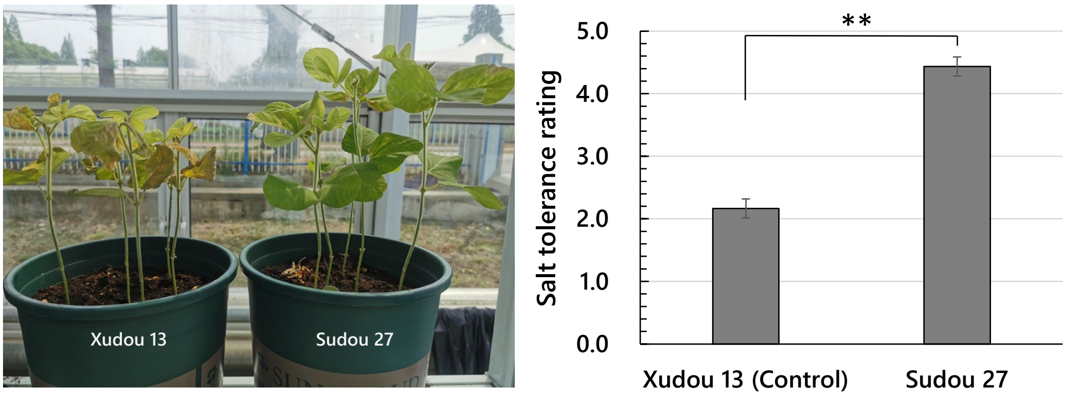

Fig. 2. Salt tolerance evaluation of "Sudou 27"

Left: Soybean plants treated with 120 mM NaCl solution for 3 weeks in seedling stage.

Right: Results of salt tolerance rating. The salt tolerance rating was classified into 5 grades, ranging from 1 (plants completely dead) to 5 (plants with normal health leaves). **: *P* < 1%.

Reference: JIRCAS Press Release (2022-09-08) *Development of New Salt Tolerant Soybean Variety with High Yield and Disease Resistance—Contributing to Stable Soybean Production in Salt-affected Agricultural Areas—*
https://www.jircas.go.jp/en/release/2022/press202207

Nitrate uptake positively correlates with phosphorus use efficiency in rice

Phosphorus (P) is one of the essential elements for plants but is frequently deficient in agricultural fields. P fertilizer is expected to be depleted in the future, and in light of the soaring cost of fertilizers, farmers cannot apply sufficient P fertilizers in many developing countries where food security is particularly threatening. Thus, for the production of rice, which is the major agricultural crop in many of these developing countries lacking ample supply of P, developing P-efficient rice variety that efficiently absorb P and/or efficiently produce biomass with limited amount of P is a promising approach. However, previous investigations suggest that P use efficiency in rice is controlled by many small-effect genetic factors, thus rendering a conventional breeding approach of limited use. Our previous metabolomics study showed that several amino acids and nitrogen (N)-containing metabolites serve as markers for P use efficiency, suggesting that N utilization might be a key for efficiency use of P. Therefore, in the current study, we examined the effect of different N sources on P use efficiency.

Addition of nitrate lowered root P concentration under low P supply compared with the condition when the same amount of N was applied solely as ammonium (Fig. 1A). This resulted in higher P use efficiency in nitrate-treated plants (Fig. 1B). Comparison of gene expression patterns in 5 rice accessions that differ in P use efficiency showed that, compared with P-inefficient genotypes such as IR64 and Taichung, P-efficient genotypes such as DJ123, Mudgo, and Yodanya had lower uptake ratio of ammonium to nitrate (Fig. 2A). Accordingly, the expression of *NRT1.1B*, which encodes a nitrate transporter that likely highly contributes to nitrate uptake, was higher in P-efficient genotypes than P-inefficient genotypes (Fig. 2B). On the other hand, the expression of *AMT1.1* that encodes one of the major ammonium transporters tended to be lower in P-efficient genotypes (Fig. 2C).

A strong positive correlation was observed between the uptake efficiency of nitrate examined under the hydroponic condition and P uptake efficiency previously examined in a low P field (Fig. 3). These observations suggest that utilization of nitrate and P are interconnected, and improvement of nitrate use may increase P use efficiency. This is in accordance with a previous hypothesis that nitrate uptake increases P solubilization in the rhizosphere and contributes to increased P uptake. Further studies are necessary to confirm if altered N fertilization scheme affects P use efficiency of rice in the field and to discover the causal gene for such genotypic differences.

(Y. Ueda, M. Wissuwa)

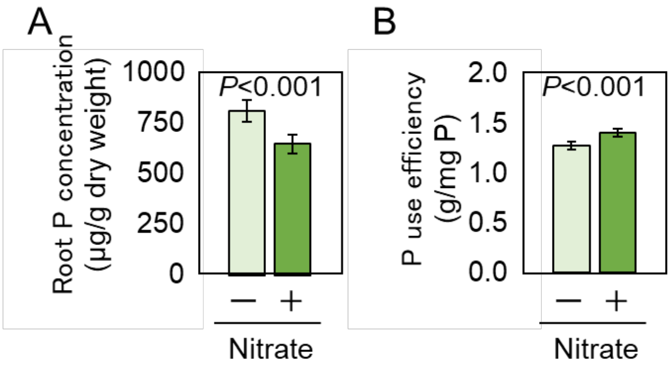

Fig. 1. Effects of nitrate on root P concentration and P use efficiency

Root P concentration (A) and P use efficiency (defined as the biomass produced per unit P) (B) of plants (cultivar: Taichung) with (+) or without (-) nitrate ion in culture solution. Mean values and standard deviations (n=4) are shown. Two-tailed Student's *t*-test was performed, and the resultant *P* value is indicated.

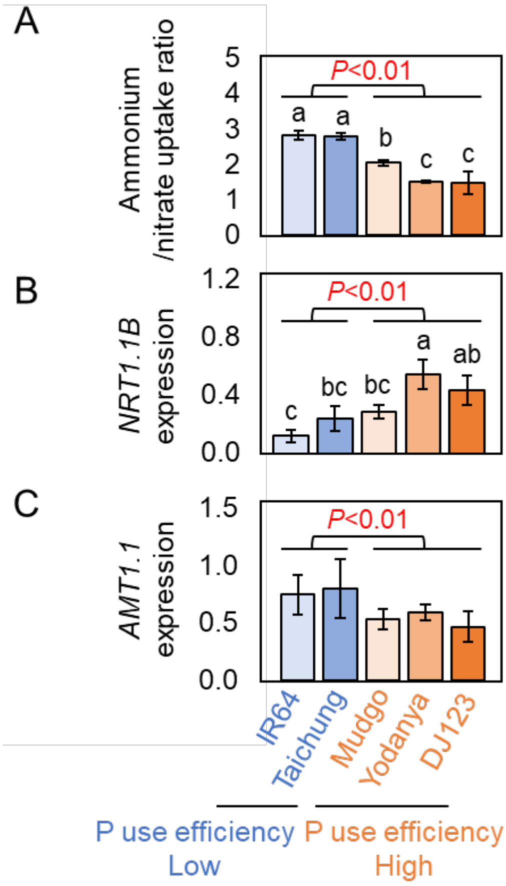

Fig. 2. N use patterns in rice accessions contrasting in P use efficiency

(A) Ratio of ammonium and nitrate uptake in roots. (B,C) The expression of *NRT1.1B* (B) and *AMT1.1* (C) in root. Mean values and standard deviations (n=4) are shown. One-way analysis of variance was performed, and the values among different genotypes were compared by Tukey-Kramer *post-hoc* test. Different alphabets indicate that the values are different at the significance level of P=0.05. Wilcoxon's rank sum test was further performed to further compare the values obtained from the groups with high or low P use efficiency, and the resultant *P* value is indicated.

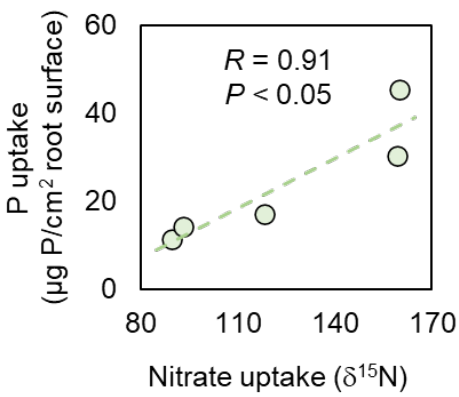

Fig. 3. Relationship between the uptake efficiency of nitrate and P

Nitrate uptake efficiency in P-limiting hydroponic condition (horizontal axis) and P uptake efficiency in P-limiting upland field (vertical axis) were compared in 5 genotypes that differ in P use efficiency. Pearson's correlation coefficient and the significance level of the correlation are indicated.

Reference: Ueda and Wissuwa (2022) *Plant and Soil* 481: 547–561.

Plant sex and flowering date are strong determinants of tuber yield in white guinea yam

White Guinea yam (*Dioscorea rotundata* Poir.) is a tuber crop widely cultivated in West Africa, accounting for more than 90% of global yam production. The average annual yield of yam has been stagnant for decades and varies from year to year. Variability in tuber yield and yield-related traits has been observed even among plants of the same variety grown in the same environment. This study focused on the sex of yam flowers as one of the causes of unstable tuber yield, as flower sex has been known to interact with tuber yield. Yams are a dioecious species, with male and female flowers on different plants (Fig. 1). Moreover, plant-to-plant variability in flower sex expression is common in yam fields. A better understanding of the relationship between flower sex and tuber yield could be crucial for genetic improvement in yam breeding.

This study used F_1-derived clonal progenies from a bi-parental cross to minimize the impact of basal genetic differences between the sex phenotypes. The impact of plant sex on agronomic traits, specifically tuber yield, was evaluated through field trials conducted for four years. The results showed that only plants with a female genotype exhibited diverse sex phenotypes (Fig. 2). Inter-plant variation in tuber yield was affected by both sex phenotype and sex genotype, but greater contribution to tuber yield was observed in the former than the latter (Table 1). Our results revealed that plants with female phenotypes had higher tuber yield than those with male phenotypes (Fig. 3). This result can be attributed to the fact that, compared to male plants, the low flowering intensity in female plants increases the availability of carbon resources for leaf development. The sexual differences in tuber yield were evident when comparing plants with similar flowering dates. Significant difference was observed for plants flowering in late July, but the difference became small for late flowering plants. This is because early flowering can avoid resource competition with tuber enlargement, which starts from mid-August.

Since sex phenotype varies with the surrounding environment in plants with the female genotype, artificial control of sex phenotype would be possible for yield improvement of female-genotyped varieties and could be achieved by appropriate field management, such as soil water control and arrangement of plant light interception, to maintain good culture conditions. The identification of the genetic factors and environmental conditions that determine flowering is currently underway, and it is expected to lead to new cultivation methods that improve tuber yield by successfully controlling flowering phenotype and flowering period, as well as the development of new varieties genetically modified for these traits.

(K. Iseki,
R. Matsumoto [International Institute of Tropical Agriculture (IITA)],
O. Olaleye [IITA], A. Asfaw [IITA])

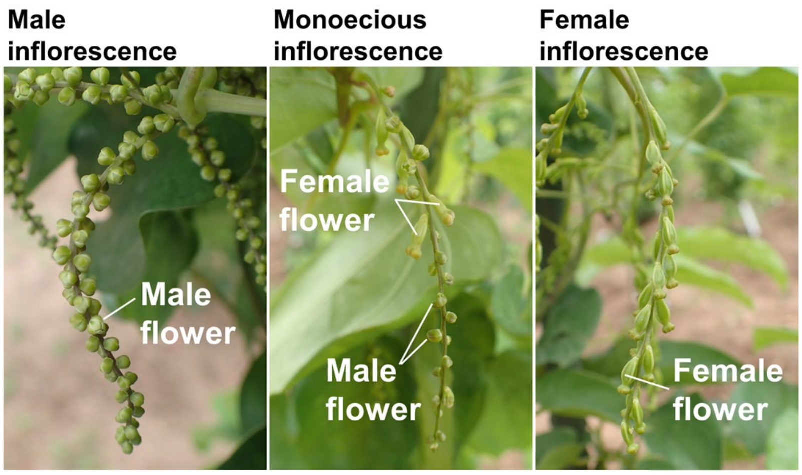

Fig. 1. Sex phenotypes in yam

Male inflorescence of male plant (left) and female inflorescence of female plant (right). Inflorescence of monoecious plant has both male flower and female flower (center).

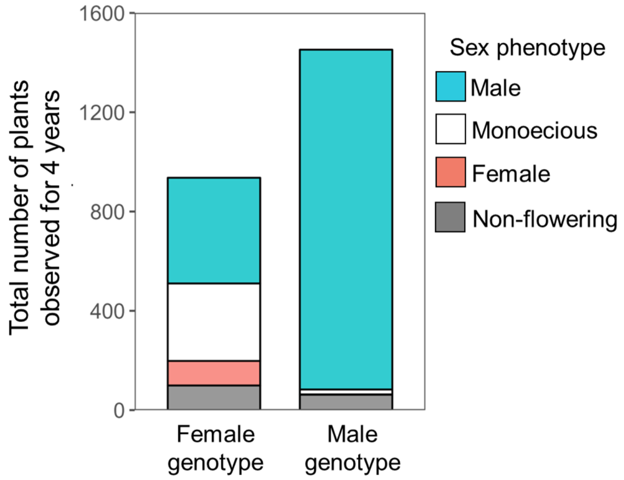

Fig. 2. Observed sex phenotype in plants with male and female genotypes

Distribution of sex phenotypes from a total of 2,400 plants, consisting of 200 accessions with 3 replications over a 4-year period. Approximately half of the plants with a female genotype showed a male phenotype.

Table 1. Effect of sex phenotype and sex genotype on tuber yield

Factor	Contribution (%)
Sex genotype	0.1 *
Sex genotype × Sex phenotype	3.2 **

The results of nested analysis of variance (ANOVA) using sex genotype as the hierarchical factor. Values indicate the contribution ratio of each factor on the total yield variation. ** and * indicate that the contribution is statistically significant at $P<0.01$ and $P<0.05$ levels, respectively.

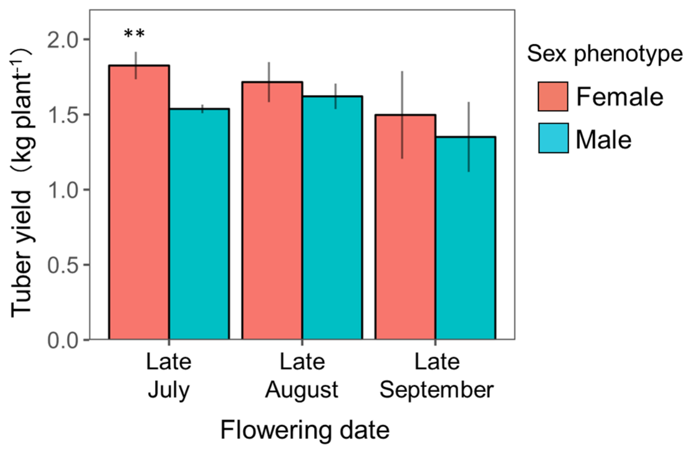

Fig. 3. Relationship between flowering date and tuber yield in plants with male and female phenotypes

Female plants had higher tuber yield than male plants when comparing plants with similar flowering dates. Significant difference at $P<0.01$ level was obtained for plants with early flowering in late July.

Reference: Iseki et al. (2022) *Frontiers in Plant Science* 13: 837951. https://doi.org/10.3389/fpls.2022.837951

Spawning season of the edible tropical oyster *Crassostrea belcheri* in the coastal area of Myeik, southern Myanmar

Oyster aquaculture research in Myanmar started in the 1970s, but commercial oyster farming techniques have not yet been established. The availability of seed oysters for oyster farming depends on the natural occurrence of juvenile oysters in coastal areas in the case of natural seedling collection. Therefore, the relationship between the environment of the target area and the spawning period of the target species needs to be clarified. In temperate regions, where water temperatures vary greatly between winter and summer, many species spawn once a year in the summer when water temperatures rise, whereas in tropical regions, where water temperatures are high all year round, they often spawn year-round. However, there is seasonal variation in the proportion of spawning individuals. The main spawning seasons have been reported as once, twice, or three times a year, and the timing may vary from region to region, even for the same species. This study aims to reveal the reproductive cycle of the edible tropical oyster *(Crassostrea belcheri)* from the waters near Myeik (Fig. 1) in southern Myanmar and to identify suitable periods for natural seedling collection of the species. From September 2017 to October 2018, 12–20 edible tropical oysters were obtained monthly from markets in Myeik (Fig. 2). Gonadal tissue sections were examined under an optical microscope, and maturity stages were determined.

The local climate is a tropical monsoon climate with a distinct dry and rainy season, with significantly higher rainfall in the rainy season. During the study period, monthly rainfall exceeded 400 mm in September–October 2017 and June–September 2018 (Fig. 3a). Histological analysis of *C. belcheri* gonads revealed that spawning occurred throughout the study period except January–March 2018, peaking at the beginning and end of the dry season in October–November and April–May, respectively (Fig. 3b, c).

The installation of collectors in the sea during the transition from dry to rainy season or from rainy to dry season is expected to increase the efficiency of natural seedling collection. Local meteorological information makes it possible to estimate the spawning season of edible tropical oysters, thus the timing of the placement of seedling collectors in the sea. However, during the rainy season, the survival and growth of juvenile oysters recruited before the rainy season would be hampered by low salinity due to freshwater inflow, etc. Further research is needed on survival and growth rates after the spawning season to establish efficient natural seedling collection techniques.

(M. Toyokawa, T. Yurimoto, Khin-May-Chit-Maung [Myeik University], H. Saito)

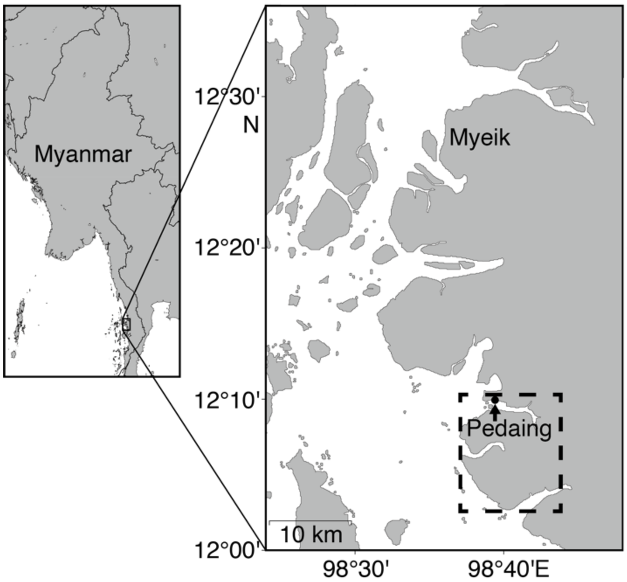

Fig. 1. Study area

The study area is located on the southernmost coast of Myanmar. Edible tropical oysters are harvested from the nearby mangrove creeks of Pedaing Village (generally within the area enclosed by the dotted line) and sold in Myeik City all year round.

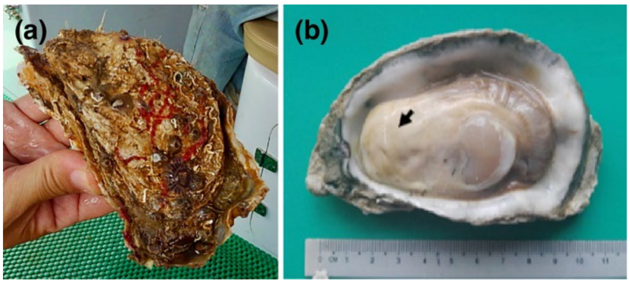

Fig. 2. Exterior of edible tropical oyster (a) and inside the shell (b)

The arrow indicates the location of the gonads.

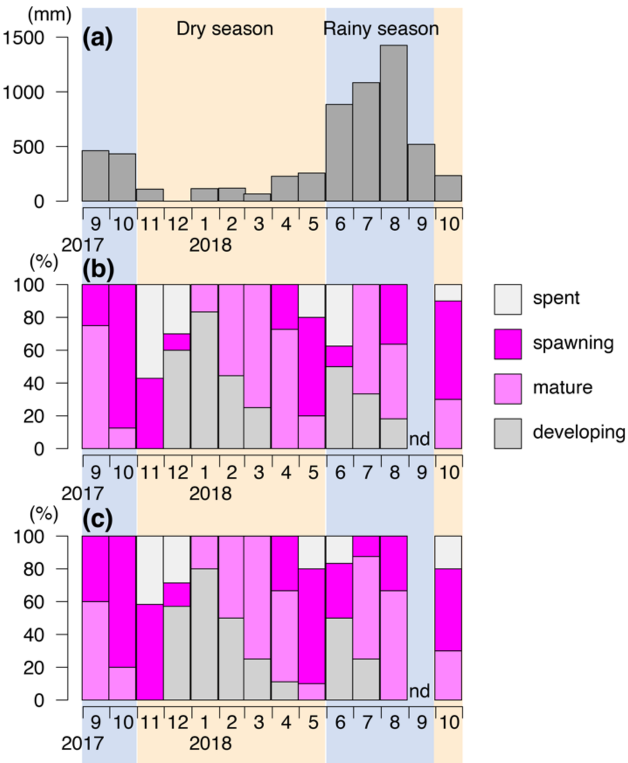

Fig. 3. Monthly precipitation in Myeik (a) and sexual maturity stages of edible tropical oysters (b, female; c, male)

The length of the rainy season varies slightly from year to year. Percentage of gonads in spawning stage is higher in October and May, which is the transition between the rainy and dry seasons.

nd: no data.

Reference: Khin-May-Chit Maung et al. (2023) *Japan Agricultural Research Quarterly* 57(3).
Figures reprinted/modified with permission.

Clarifying the genetic diversity of *Amaranthus tricolor* 'Hiyuna,' a traditional Asian vegetable

Amaranthus tricolor L., called 'hiyuna' in Japanese, is used as a traditional leafy vegetable in Asia. *A. tricolor* is resistant to major diseases, is more tolerant to environmental stresses, and is a rich source of nutrients such as iron and calcium, as well as vitamin C and beta-carotene. Yet despite this diversity and excellent nutritional quality, breeding of improved cultivars is widely neglected in modern breeding. *A. tricolor* accessions are conserved in the World Vegetable Center (WorldVeg) genebank (https://avrdc.org) and in the USDA National Plant Germplasm Information System (https://www.ars-grin.gov). These accessions hold a wide variety of genetic variations and useful agronomic traits with a high potential for breeding improved cultivars (Fig. 1). Some studies have reported on the evaluation of *A. tricolor* genetic resources, but the diversity conserved in both genebanks has not yet been systematically evaluated.

In this study, we evaluated the genetic diversity in the collection of *A. tricolor* accessions conserved by the WorldVeg and USDA genebanks based on genome-wide single-nucleotide polymorphisms (SNPs) developed using double-digest RAD-Seq (ddRAD-Seq), and created a core collection, which is valuable in improving crop breeding programs for performing extensive evaluations with minimal materials.

We analyzed the genetic diversity and population structure among 465 *A. tricolor* accessions with SNPs developed by ddRAD-Seq. We identified a set of 5,638 SNPs without missing data in 440 accessions in order to establish a breeding platform. We analyzed genetic diversity by principal coordinate analysis (PCoA) of the accessions using this marker set. The 377 *A. tricolor* accessions clustered into 4 main subpopulations (Q1–Q4) and an admixture group (Fig. 2). The proportion of accessions from India, Bangladesh, and China in Q1, Q2, and Q3 was significantly higher than that in other countries, and the proportion of the admixture group in all accessions was highest in accessions from Southeast Asia, especially Indonesia and Malaysia (Fig. 3). In addition, we created a core collection of 105 accessions representing the genetic diversity of 377 source accessions. This core collection is available for research and breeding through the WorldVeg genebank.

Marker selection breeding using the SNP markers and core collection obtained this time will pave the way for the development of breeding techniques and new varieties to improve nutritional value, eating quality, and yield. It is also expected to contribute to sustainable vegetable production in tropical and subtropical regions.

(K. Hoshikawa,
Y. Yoshioka [University of Tsukuba], K. Shirasawa [Kazusa DNA Research Institute])

Fig. 1. Phenotypes of *A. tricolor* accessions cultivated at World Veg

The photos exhibit phenotypic diversity, including leaf color, shape, and height. We cultivated 465 *A. tricolor* genetic resources.

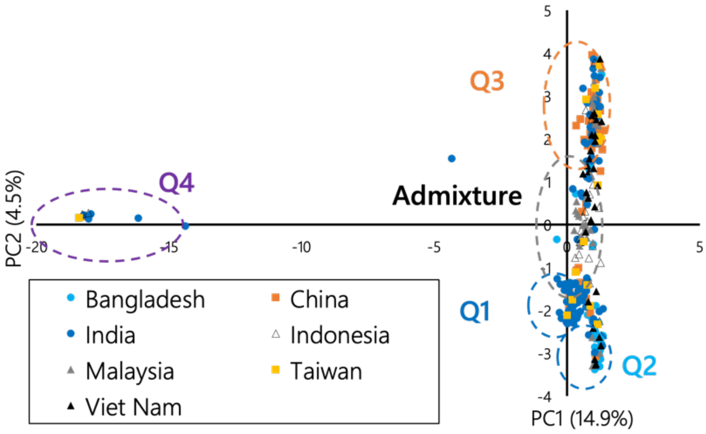

Fig. 2. Principal coordinate analysis (PCoA) of *A. tricolor* accessions based on genome-wide SNPs

Seven countries from which at least 10 accessions are derived are shown. The plots are colored to illustrate the origin of the accessions and to show the clustering according to population structure and geography.

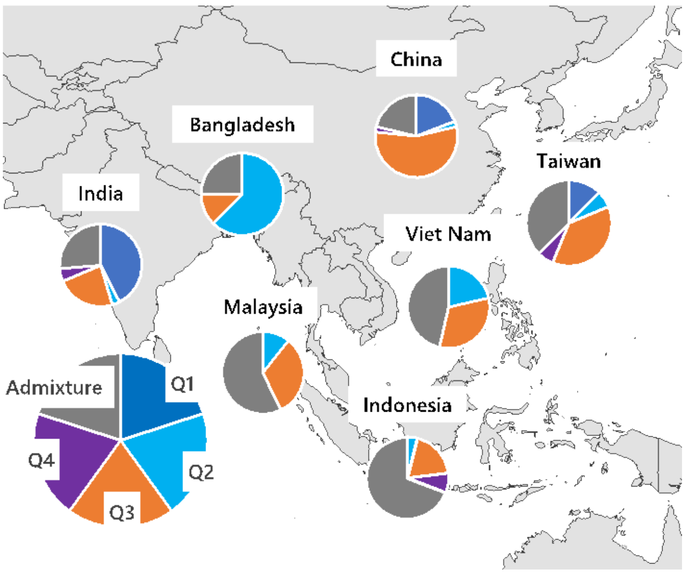

Fig. 3. Classification and geographic distribution of *A. tricolor* genetic resources using SNP markers

The pie graphs show the proportions of accessions of specific subpopulations in each country.

Reference: Hoshikawa et al. (2022) *Scientia Horticulturae* 307: 111428.

Selection of a promising donor for developing zinc-biofortified rice based on genomic prediction model

Increasing zinc (Zn) concentrations in edible parts of food crops, an approach termed Zn-biofortification, is a global breeding objective to alleviate micro-nutrient malnutrition. In particular, infants in countries like Madagascar are at risk of Zn deficiency because their dominant food source, rice, contains insufficient Zn. Biofortified rice varieties with increased grain Zn concentrations would offer a solution and our objective is to explore the genotypic variation present among rice gene bank accessions and verify their performance under farmers' field conditions. A training set of 253 rice accessions was grown at two field sites in Madagascar. A genomic prediction model was developed from the above training set to predict brown rice Zn concentrations of 3,024 sequenced rice accessions. Predicted concentrations ranged from 17.1 to 40.2 ppm Zn with significant differences among rice sub-populations, of which *aus* group (n=201) had highest Zn concentrations (Fig. 1). The prediction accuracy of the developed model was evaluated using 61 previously untested accessions, and the relatively high coefficient of determination (R^2=0.55) between measured and predicted values confirmed the model validity (Fig. 2). Very high predicted grain Zn concentrations of accessions belonging to the *aus* sub-species were confirmed in additional field experiments, with one potential donor (IRIS313-9368) having more than twice the grain Zn compared to a local check variety (X265) (Fig. 3). We conclude that utilizing donors from the *aus* sub-species and employing genomic selection during the breeding process are the most promising approaches to raise grain Zn concentrations in rice.

(M. Wissuwa, Y. Tsujimoto, J. Tanaka,
M. Rakotondramanana [The National Center for Applied Research on Rural Development (FOFIFA)],
R. Tanaka [University of Tokyo],
J. Stangoulis [Flinders University], C. Grenier [The French Agricultural Research Centre for International Development (CIRAD)])

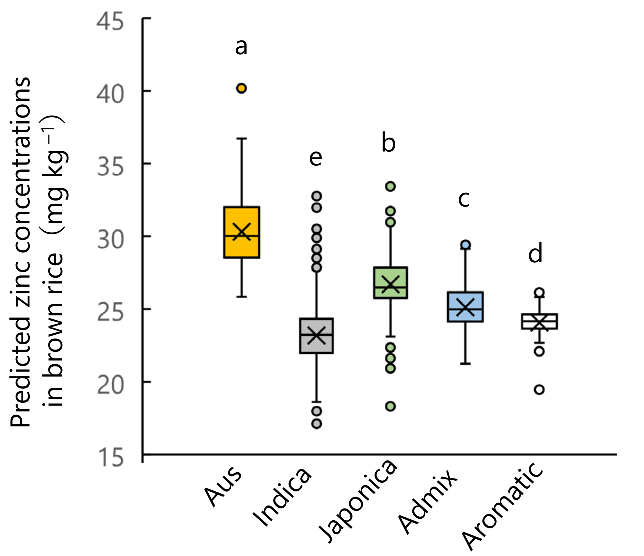

Fig. 1. Predicted variations in brown rice zinc concentrations of 3,024 accessions from five rice sub-populations

Aus (n=201); Indica (n=1,089); Japonica (n=855); Admix (n=103); Aromatic (n=76). Different alphabets indicate significant differences in the means (shown in ×) among sub-populations by Tukey's HSD at *P*<0.05. The sub-populations were categorized by IRRI genebank.

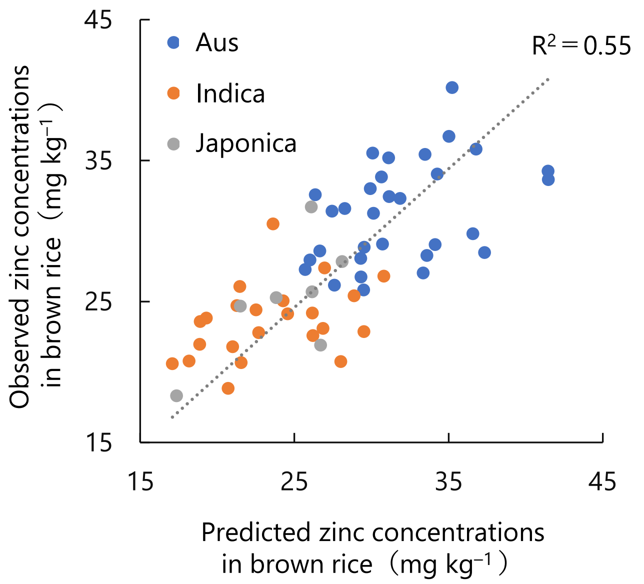

Fig. 2. Relationship between observed and predicted brown rice zinc concentrations of 61 unseen accessions

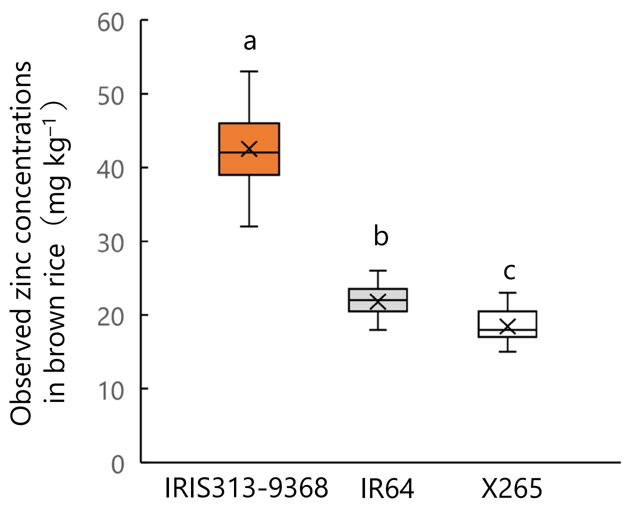

Fig. 3. Observed brown rice zinc concentrations of three rice accessions across 10 different growth conditions

IRIS313-9368: the aus type predicted to have high Zn concentration; IR64: a popular high-yielding lowland variety in the tropical region; X265: a leading lowland variety in Madagascar. Different alphabets indicate significant differences in the means (shown in ×) among sub-populations by Tukey's HSD at *P*<0.05.

Reference: Rakotondramanana et al. (2022) *Theoretical and Applied Genetics* 135: 2265－2278.

Increased lowland rice yield improves nutrition of farmers in Madagascar

Sub-Saharan Africa has the highest rate of hunger in the world, accompanied by serious micronutrient deficiencies. Since low agricultural productivity of staple crops is a major challenge in this region, increasing crop yield is urgently needed and expected to increase farmers' energy intake and cash income. Agriculture is said to have an effect on farmer’s nutrition; however, only a few studies have evaluated the impact of increased productivity of staple food crops on farmers' nutritional supply in rural areas of Sub-Saharan Africa. To explore the pathways and effects of lowland rice yield on farmers’ nutrient supply, we monitored the agricultural production and food consumption of 600 households over a three-year period from 2018 to 2020 in the rural areas of Madagascar, where rice is the main staple food.

We found that the elasticities of energy, zinc, iron, and vitamin A with respect to lowland rice yield are significantly positive (Fig. 1). Higher lowland rice yield increases the supply of these nutrients, for which deficiencies are particularly widespread in the target area. We also showed that an increase in rice yield leads not only to rice consumption but also to cash revenue from rice sales (Table 1). Increased cash revenue accelerates purchases of nutritious foods such as vegetables, fruits, and meat & fish at the market (Fig. 2). While yield has a significant positive impact on whether rice is sold (Yes/No), the interaction term of yield and distance to the main road has a significant negative impact (Table 2). Good market access promotes rice sales, suggesting the importance of the role that the market plays. This pathway is illustrated in Figure 3. In addition to increasing rice consumption (red line in Fig. 3), higher productivity of lowland rice increases purchases of nutritious foods through market channels (blue line in Fig. 3). Therefore, improving lowland rice productivity is effective in improving farmers' nutrition in terms of both quantity (energy supply) and quality (nutrition balance including micronutrients).

These findings contribute to the formulation and implementation of measures to improve nutrition by increasing the productivity of staple crops grown in rural areas of Sub-Saharan Africa. Technological interventions aimed at increasing the productivity of staple crops are effective in improving the nutrition of poor farmers and, in turn, SDG Goal 2 (Zero Hunger). This is the result of diversifying purchasing behavior through the market as well as through self-consumption, and it is necessary to ensure farmers' access to the market along with technology adoption.

(S. Shiratori, R. Ozaki,
N.A. Nikiema [University of Tokyo], T. Sakurai [University of Tokyo],
J. Rafalimanantsoa [National Office of Nutrition, Madagascar])

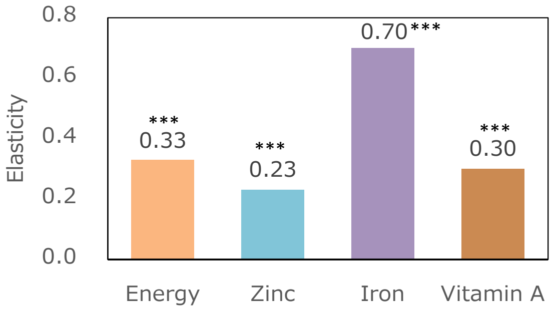

Fig. 1. Elasticities of lowland rice productivity on nutrient supply
***: Significant at 1% level

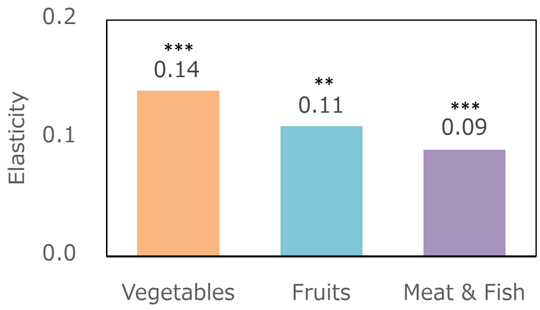

Fig. 2. Elasticities of cash revenue from lowland rice sales on food expenditure
***, **: Significant at 1% & 5% levels, respectively

Table 1. Elasticities of lowland rice yield on rice consumption and on cash revenue from rice sales

Consumption	Cash Revenue
0.20***	0.41***

***: Significant at 1% level

Table 2. Effects of lowland rice yield and distance to the main road on rice commercialization

Yield	Yield * Distance (ln)
0.16***	–0.08***

***: Significant at 1% level

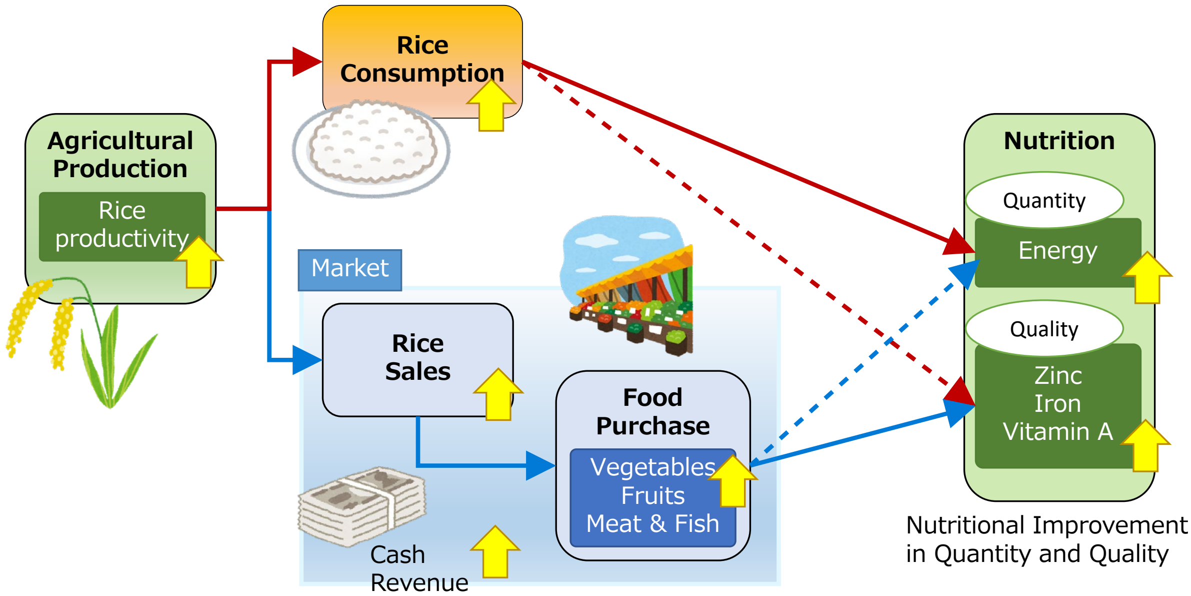

Fig. 3. Linkage from agricultural production to farmers' nutritional supply
Pathway (red): Increased rice productivity leads to an increase in self-consumption of rice, contributing to nutritional improvement mainly in terms of quantity.
Pathway (blue): Increased rice productivity increases rice sales and hence cash revenue from that. It leads to an increase in purchase of nutritious foods, which contributes to nutritional improvement mainly in terms of quality.
Solid-line and dashed-line arrows indicate major and secondary contributions, respectively.

Reference: Nikiema et al. (2023) *Food Secur.* https://doi.org /10.1007/s12571-022-01333-5

Mitigating income stagnation and volatility in African smallholder agriculture using small reservoir irrigation technology and stochastic programming model

Due to the precarious nature of rainfed crop production, smallholder farmers in Africa are confronted with the peril of insufficient and unstable income (hereinafter referred to as "risk"). While irrigation has been recognized as a means of mitigating this risk, irrigation plans that are well-suited for farmers' risk management are seldom explored. This study introduces a farm management planning model that integrates the production of irrigated crops utilizing a small reservoir with that of rainfed crops. This model is based on the results of a participatory on-farm trial and survey conducted over a five-year period in northern Ghana. Using stochastic programming, the model considers the variability of crop yields, prices, and costs under the prevailing farm, water, and social conditions in order to identify the most effective irrigation cropping patterns that enhance and stabilize income (Fig. 1).

The model analysis revealed three distinct types of optimal cropping based on the level of risk and income: minimal risk, actual risk, and maximal income. To minimize risk, pepper production, which is highly profitable but risky, should be reduced, and rice and leafy vegetables should be grown instead, using a small reservoir. If farmers can tolerate the actual level of risk in rainfed agriculture, it is suggested that they decrease maize production, the primary staple, to a self-sufficient level and expand irrigated rice and leafy vegetable production, which could result in a 60% increase in expected income. Reducing rainfed rice production to a level that enables rice self-sufficiency and increasing pepper production will maximize expected income. Although risk will increase, the income level is expected to exceed that of rainfed agriculture even in the case of a downturn in income (Fig. 2). Note that the investment in irrigation facilities is difficult to recoup in the "minimal risk type" due to the limited increase in expected income. The "maximal income type" can recoup its investment in approximately four years, while the "actual risk type" can do so in approximately eight to twelve years (Fig. 3).

To facilitate the improvement of local cropping systems, a program called BFMgh has been developed to create enhanced farming plans for smallholders in Ghana. The program stores sample data on irrigated and rainfed crops collected during this study and is available on the JIRCAS website. In northern Ghana, attention should be given to potential conflicts over reservoir water usage as some individuals may seek to utilize a portion of the reservoir water for domestic purposes, even if it was constructed for agricultural purposes.

(J. Koide, S. Yokoyama, S. Hirouchi, N. Oka, C. Hirose, S. Yanagihara, M. Oda, W. Oishi [University of Tsukuba])

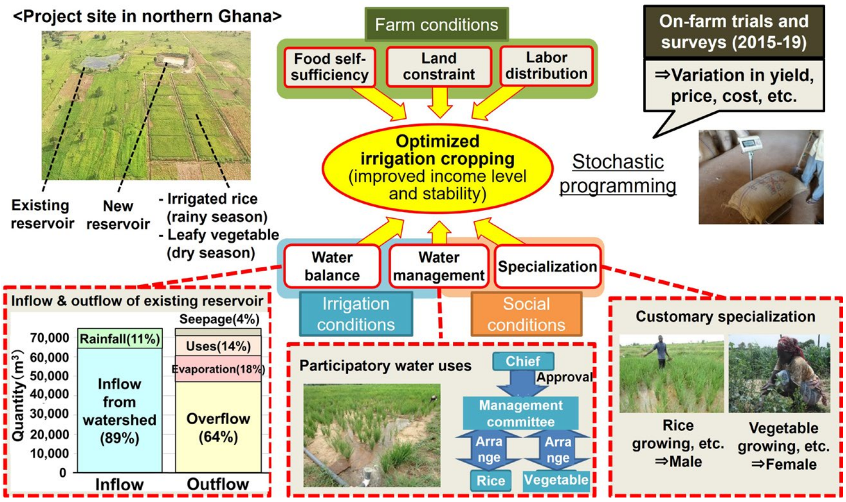

Fig. 1. Schematic diagram of the constructed model

Water allocation to irrigated crops will be optimized based on the available water capacity of the newly constructed reservoir designed to store excess water from the existing reservoir.

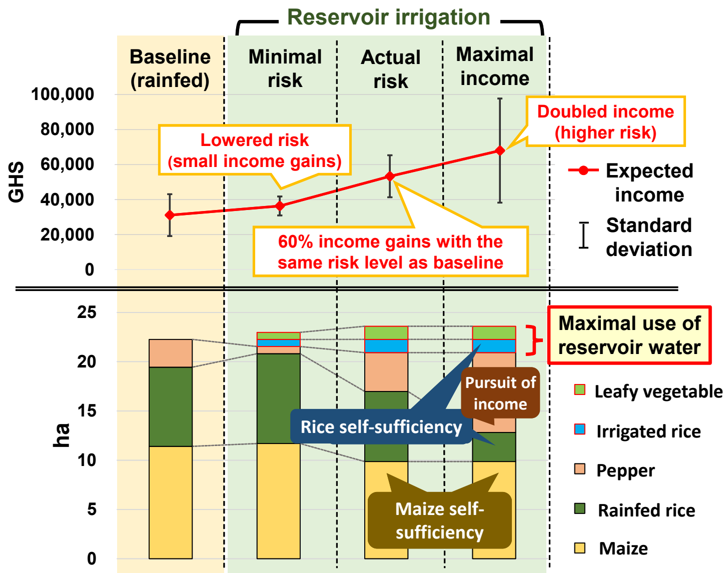

Fig. 2. Optimal cropping plan (below) and its income enhancing and stabilizing effect (above)

The results of model analysis for 30 irrigated farmers using the new reservoir (water storage capacity: 5000 m^3) constructed at a project site in northern Ghana are shown.

The risk denotes the standard deviation of income (bars in the figure).

GHS: Ghanaian Cedi

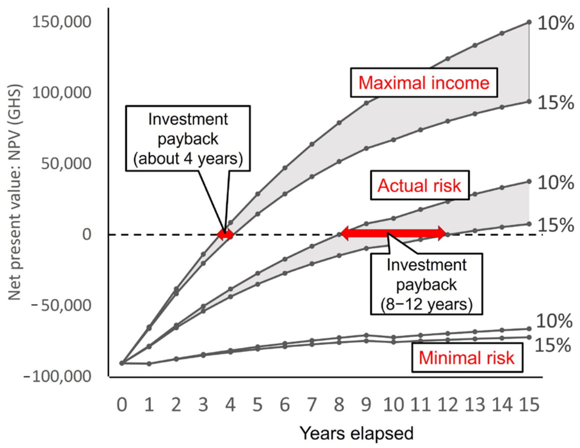

Fig. 3. Return on investment according to optimal cropping plan and discount rate (10% – 15%)

NPV: the present value of the expected income from each optimal cropping plan minus the investment cost for irrigation facilities (95,624 GHS).

The intersection with zero is the number of years required for investment payback (red arrow in the figure). It varies slightly depending on the discount rate.

GHS: Ghanaian Cedi

References: 1) Koide et al. (2021) *Agric. Syst.* 191: 103149. https://doi.org/10.1016/j.agsy.2021.103149
Figures reprinted/modified with permission.
2) "BFMgh: Program for creating Improved Farming Plans for African Smallholders" (2022)
https://www.jircas.go.jp/ja/database/farm_management_model_for_shfa

Phosphate rock-enriched compost with rhizosphere soil increases sorghum yield equivalently to chemical fertilizers

The limited availability of phosphorus in sub-Saharan African soils is a significant constraint to agricultural production. Cereal production in the area is only 1.59 tons per hectare, while the world average is 4.15 tons per hectare (World Bank, 2021). In view of the demographic trend showing high population growth in sub-Saharan Africa, increasing crop production by improving soil nutrient availability is of high priority. Unfortunately, the recent surge in the prices of chemical fertilizers complicates their effective use by smallholder farmers. Therefore, in a previous study, we formulated a new compost type by co-composting crop residue with low-grade phosphate rock and soil collected from the sorghum root rhizosphere area (S-PrCo). The rhizosphere soil, influenced by complex molecular exchanges between roots and microbes via root exudates, is generally rich in beneficial microbes, including phosphorus solubilizers. We included a phosphate rock-enriched compost without rhizosphere soil (PrCo) and compost with only crop residues (Co). All composts were made with 100 kg of sorghum straw as crop residue and 460 g of urea to reduce the C/N ratio from 55/1 to 25/1 and ease the decomposition. We added 10 kg of phosphate rock and 10 kg of rhizosphere soil where necessary. Each compost pile was arranged in five successive layers, the moisture content was adjusted to 65%, and the composting lasted 180 days (Fig. 1). The available phosphorus and phosphate-solubilizing microbes increased in S-PrCo.

The present study evaluated S-PrCo, PrCo, and Co on sorghum growth and soil properties compared to the chemical fertilizer NPK (nitrogen-phosphorus-potassium). The results showed that S-PrCo significantly increased sorghum dry matter (grain, stem/leaf/ear) compared to PrCo and Co and gave a yield equivalent to the chemical fertilizer (Fig. 2). S-PrCo also improved soil biological properties by increasing the population of arbuscular mycorrhizal fungi involved in the uptake and transfer of phosphorus to the roots. It also enhanced the abundance of P-cycling microbes, such as phosphate-solubilizing bacteria with the glucose dehydrogenase (*gcd*), acid phosphatase (*aphA*), phosphonatase (*phnX*), and phosphate specific transporter (*pstS*) genes as shown in Figure 3. The study clarified that the significant yield-increasing effect of the new compost type (S-PrCo) is not only due to the increase of available phosphorus in the compost prior to application but also due to the improvement of soil biological activity with the promotion of phosphorus solubilization and absorption during the cultivation period. S-PrCo also improves soil chemistry by correcting the soil pH. This research indicates that co-composting crop residues with low-grade phosphate rock and rhizosphere soil is expected to provide farmers in sub-Saharan Africa with a new fertilizer option against rising chemical fertilizer prices and soil degradation.

(P.S. Sarr)

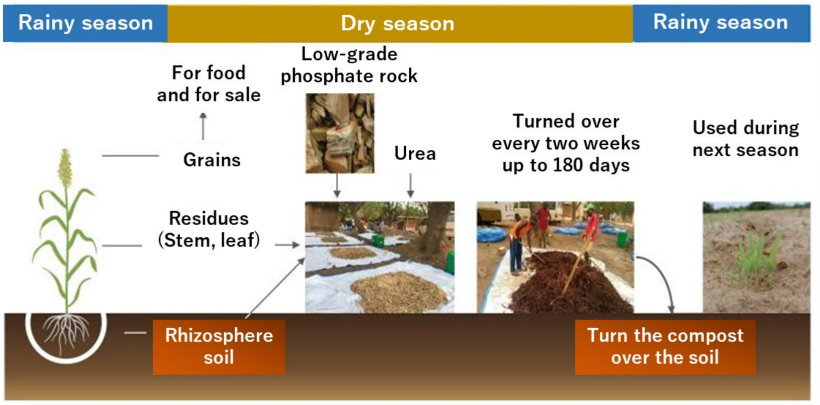

Fig. 1. Conceptual diagram of the utilization of phosphate rock-soil-enriched compost

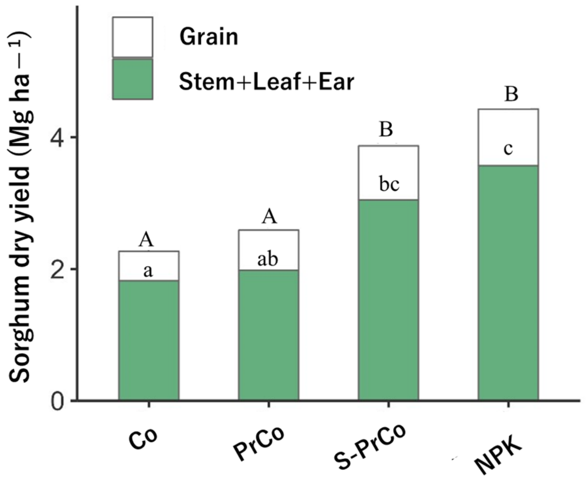

Fig. 2. Fertilization effect of phosphate rock soil-enriched compost

*Co: residue compost, PrCo: phosphate rock-enriched compost, S-PrCo: phosphate rock-soil-enriched compost, NPK: commercial NPK fertilizer

*Different alphabet capital letters between treatments show significant differences in total dry matter yield (grain plus sum of stem-leaf-ear). Different alphabet lower case letters show significant differences in grain yield

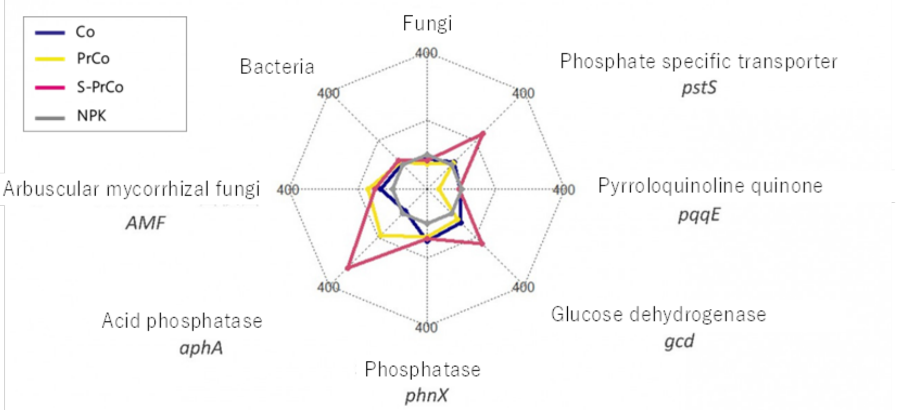

Fig. 3. Amount of effective microbes in rhizosphere soil during sorghum growth

*Co: residue compost, PrCo: phosphate rock-enriched compost, S-PrCo: phosphate rock-soil-enriched compost, NPK: commercial NPK fertilizer

*Shown as a relative value (%) with the case of applying imported chemical fertilizer NPK (gray in the figure) as 100%

*Arbuscular mycorrhizal fungi (AMF), glucose dehydrogenase (gcd), and phosphate-specific transporter-producing microbes (pstS) show the values at 52 days after seeding, which is the early stage of growth

* For other items, average values for 52 days, 93 days, and 115 days after seeding are shown.

References: Sagnon et al. (2022) *Scientific Reports,* https://doi.org/10.1038/s41598-022-18318-1.
Sarr et al. (2020) Frontiers in Environmental Science, doi:10.3389/fenvs.2020.559195

Figures reprinted/modified with permission.

A curve number estimation model to accurately calculate reservoir inflow

There are many reservoirs in Northern Region, Ghana (Fig. 1). The reservoirs overflow during the rainy season, and the overflowing water flows into rivers without being used downstream. If the overflowing water can be used for irrigation, agricultural productivity is expected to increase. To utilize overflow water for irrigation, it is necessary to estimate the volume of water that flows out of the watershed when rain falls (runoff). The curve number method calculates the volume of runoff from the watershed using the curve number (CN), rainfall, and watershed area (Fig. 2). Using standard CN (Fig. 3, Standard CN), observed runoff per rainfall could not be presented (NSE = −4.46), and the difference with the observed runoff was large during the whole period (Fig. 3). This study proposes a CN estimation model to calculate runoff with accuracy and practicality.

To approximate the observed runoff, a model was devised to estimate CN by multiple regression analysis, using CN calculated backwards from the observed runoff for each rainfall as the objective variable; and daily rainfall, dry period, and hourly maximum rainfall as explanatory variables. Of the devised models, the method of estimating CN using daily rainfall (log-transformed), number of days in a dry period, and hourly maximum rainfall (Method (1)) had the best reproducibility with an average NSE of 0.74. In districts where hourly rainfall data are difficult to obtain, Method (2), which estimates CN using only daily rainfall (log-transformed) and the number of days in a dry period (NSE=0.51), is recommended. Also, methods (1) and (2) show a small difference between the observed and the calculated runoffs for the whole period (Fig. 3). Using CN estimated by these methods, runoff per rainfall can be calculated, and from the calculated runoff and the water balance equation, the volume of water that overflows (Fig. 4), i.e., when the water level in the reservoir exceeds 2.1 m, can be calculated. Applying Method (1) to 2017, it can be calculated that 5,890 m^3 of overflow water was generated from the reservoir (Fig. 5). The CN estimation model devised in this study can estimate runoff using only rainfall and can be used in developing regions with data scarcity.

The “Supplementary Irrigation Manual for Rice Production Using Small Reservoirs,” which describes a method of using overflow water for irrigation in rice farming, is available on the JIRCAS website. The results of this study are based on model calculations for one of the many reservoirs in Northern Region, Ghana, hence the regression coefficients will need to be recalculated for application to other reservoirs.

(C. Hirose, S. Hirouchi, M. Yamada, N. Oka, H. Furihata, H. Horino [Osaka Metropolitan University])

Fig. 1. Bird's-eye view of the reservoir

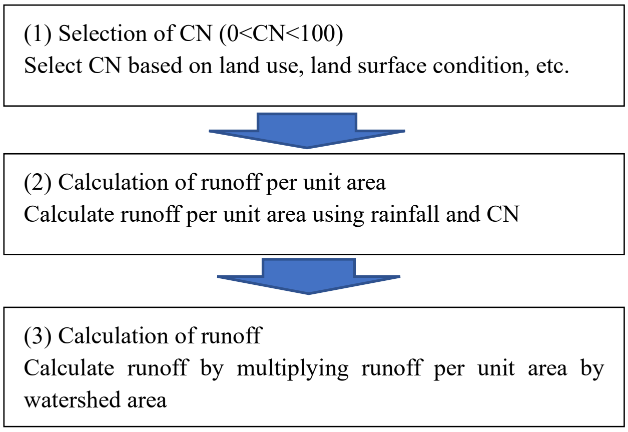

Fig. 2. How to calculate runoff using the CN method

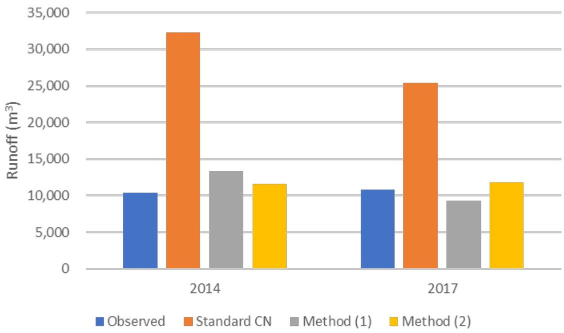

Fig. 3. Observed and calculated runoffs

Method (1) y = -13.38lnx1-0.362x2+0.407x3+116.741

Method (2) y = -8.718lnx1-0.448x2+109.305

where

y: estimated CN, x1: daily rainfall (mm), x2: number of days in a dry period (d), x3: hourly maximum rainfall (mm)

Calculation period: from the start of water storage till the start of water overflow

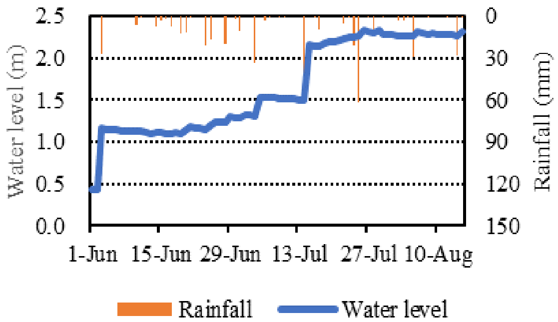

Fig. 4. Water levels and daily rainfall in the reservoir (2017)

When the water level in the reservoir exceeds 2.1 m, overflow occurs.

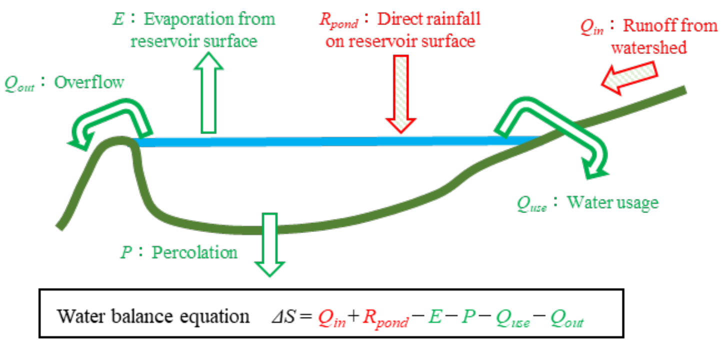

Fig. 5. Annual water balance of the reservoir calculated using reservoir water balance components, water balance equation, and Method (1) (2017)

Q_{in} : 21,229 m^3, R_{pond} : 3,950 m^3

E : 9,017 m^3, P : 6,063 m^3

Q_{use} : 4,035 m^3, Q_{out} : 5,890 m^3

ΔS : 174 m^3

where ΔS: Change in storage content of reservoir (m^3/d), Q_{in}: Runoff from watershed (m^3/d), R_{pond}: Direct rainfall on reservoir surface (m^3/d), E: Evaporation from reservoir surface (m^3/d), P: Percolation (m^3/d), Q_{use}: Water usage (domestic and livestock use) (m^3 /d), Qout: Overflow (m^3/d)

Reference: Hirose et al. (2022) *IDRE Journal* No. 314 (90-1): II _29– II _41.
Figures 4 and 5 reprinted/modified with permission.

Development of "Doncella INTA-JIRCAS," a new soybean variety with high Asian soybean rust resistance

Asian soybean rust (ASR) is a serious soybean disease that accelerates defoliation and reduces yield of soybean. Farmers have been using fungicides for ASR control, but the fungicide resistance of the pathogen is increasing. The use of resistant varieties would reduce production cost and environmental impact by limiting the excessive use of fungicides. Resistance genes (*Rpp*s) to ASR have been identified in soybean. In addition, JIRCAS has shown that soybean plants with multiple *Rpp* genes are not only resistant to many strains of the ASR pathogen with different virulence, but also show a high level of resistance to them. In this study, we developed a soybean variety with high ASR resistance adapted to Argentina, using the *Rpp*-pyramided lines bred by JIRCAS.

We crossed the ASR-resistant line "No6-12-1," which has three resistance genes (*Rpp2*, *Rpp4*, and *Rpp5*) developed by JIRCAS, as a non-recurrent parent and the variety "INTA ALIM5.09" from the National Agricultural Technology Institute (INTA), as a recurrent parent. The F_1 individuals were then backcrossed to the recurrent parent, and individuals carrying the three resistance genes were selected using DNA markers. This process was done continuously, and the line with the best production characteristics was selected and registered in the National Seed Institute (INASE) of the Ministry of Agriculture, Livestock and Fisheries of Argentina as "Doncella INTA-JIRCAS." The official date of registration of the new soybean variety was April 25, 2022 (Variety Registration Number: 4304). The new variety was similar to the recurrent parent, INTA ALIM5.09, for major soybean traits such as stem termination (Table 1). However, ASR severity on the leaves in the field experiment was less than 1% for the new variety, compared to more than 30% for the recurrent parent, INTA ALIM5.09 and the reference varieties, INTA Paraná 629 and INTA Paraná 5500, indicating that the new variety has high ASR-resistance derived from "No6-12-1" (Fig. 1).

Because both infection and spore production of ASR are suppressed in the new variety (Fig. 1), fungicide use can be significantly reduced. Actually, soybean varieties developed in Paraguay by introducing the same gene combinations have yielded 1.4- or 1.7-fold higher than pre-improved varieties under fungicide-free conditions. However, in order to maintain the resistance of new varieties for a long time, it is necessary to suppress the emergence of new ASR pathogens that can break the resistance, so fungicides should be used in appropriate quantities and frequencies.

(N. Yamanaka,
A. De Lucia [National Agricultural Technology Institute],
M. Heck [National Agricultural Technology Institute])

	New variety	Reference variety 1 (Recurrent parent)	Reference variety 2	Reference variety 3
Name of variety	Doncella INTA-JIRCAS	ALIM5.09	INTA Paraná 629	INTA Paraná 5500
Severity (%±SD)	Less than 1	37.3±1.1	46.2±4.0	50.8±1.1
Sporulation level	0	3	3	3
Infected leaves				

Fig. 1. Severity and resistance of a new soybean variety and reference varieties to Asian soybean rust

Severity (% area of lesions) and resistance (sporulation level 0–3 on lesions) of new variety: Doncella INTA-JIRCAS and the reference varieties for registration: INTA ALIM5.09 (recurrent parent), INTA Paraná 629, and INTA Paraná 5500. Results of trials in INTA-Cerro Azul Experimental Station, Argentina.

Table 1. Major characteristics of new soybean variety and reference varieties

	New variety	Reference variety 1 (Recurrent parent)	Reference variety 2	Reference variety 3
	Doncella INTA-JIRCAS	**ALIM5.09**	INTA Paraná 629	INTA Paraná 5500
Stem termination	Indeterminate	Indeterminate	Indeterminate	Indeterminate
Flower color (hypocotyl color)	Purple	Purple	Purple	Purple
Pubescence color (stem and pod)	Gray	Gray	Gray	Gray
Leaflet shape	Oval	Oval	Oval	Oblong
Seedcoat color	Yellow	Yellow	Yellow	Yellow
Hilum color	Yellow	Yellow	Light brown	Black
Growth period	104 days	107 days	119 days	121 days
Plant height	69.4 cm	69.1 cm	93.8 cm	87.5 cm
100-seed weight	18.5 g	21.1 g	15.2 g	11.9 g
Seed lipid content [1]	23.1%	22.6%	23.5%	23.4%
Seed protein content [1]	40.5%	40.9%	35.6%	34.0%
Stem canker resistance	Moderately resistant	Moderately resistant	Resistant	Resistant
Asian soybean rust resistance	**Resistant**	**Susceptible**	**Susceptible**	**Susceptible**
Herbicide resistance	Susceptible	Susceptible	Susceptible	Resistant
Yield (t/ha) in INTA experimental stations [2]				
2018 – 2019 Cerro Azul	1.7667	1.7778	1.8326	1.8289
2018 – 2019 Parana	3.9286	4.0715	4.5631	3.8447
2018 – 2019 Marcos Juarez	3.5929	3.8782	4.0828	3.0326
2017 – 2018 Cerro Azul	2.7370	2.9699	2.8815	2.6359
2017 – 2018 Parana	2.5236	1.6240	2.1481	2.0371

[1] Seed protein and lipid content are averages from the Marcos Juarez and Parana experimental stations.

[2] The significance levels (5%) for a total of five yield data for two years at three locations are 0.2686, 0.5281, 0.5043, 0.7936, and 0.4001 (t/ha) from top to bottom.

References: Variety registration in INASE (number: 4304 and date: April 25, 2022).
Kato et al. (2022) *Tropical Plant Pathology* 47: 599–607.
Yamanaka and Hossain (2019) Plant Breeding 138: 686–695.
Data in Figure 1 and Table 1 taken from the application for variety registration.

Japan International Research Center for Agricultural Sciences

Headquarters (Tsukuba)
1-1 Ohwashi, Tsukuba, Ibaraki
305-8686, JAPAN
TEL : +81-29-838-6313
FAX : +81-29-838-6316

Tropical Agriculture Research Front (TARF)
1091-1 Maezato-Kawarabaru, Ishigaki
Okinawa, 907-0002, JAPAN
TEL : +81-980-82-2306
FAX : +81-980-82-0614

https://www.jircas.go.jp/